The Meteorological Magazine

October 1993

Mediterranean squall
Modelling ocean waves
Wave cloud
Orographic cirrus
World weather news — July 1993

HMSO

Met.O.1010 Vol. 122 No. 1455

The Meteorological Magazine

October 1993
Vol. 122 No. 1455

551.515.8(449.45)

A Mediterranean squall

D. Senequier
Ingénieur Divisionnaire des Travaux de la Météorologie
Centre Météorologique, Interrégional du Sud Est, Marignane, France

Foreword by R.M.Blackall

I took a holiday in Calvi, Corsica, in 1992. One afternoon the 2/8 Sc drifting over on the moderate SW wind started to become more extensive and they passed by increasingly quickly as the pressure fell. At about 2130 local time there was a sudden violent squall and torrential rain that lasted for about five minutes. On my return to England I wrote to Météo-France asking if they could tell me what had happened. What follows is a précis translation of the fat report that eventually arrived: it is obvious that the forecasts from Bastia (see page 233) were not listened to by some of the locals in Calvi who had assured me there were no storms about.

I have provided an outline map of the island showing places named in the text, but an atlas should be referred to to understand the steep topography that constrains the wind direction. An example is that the 3.5 km between Calvi and Ste. Catherine airport was associated with a change of almost 90° in wind direction on 1 September.

Preface

The meteorology of the Mediterranean is characterized by two dangerous traits, violence and rapid development, of which aviators, mariners and businesses must be wary, especially during sensitive operations such has heavy lifts and oil-rig work. The natives are accustomed to the climate and notice the signs and portents, but they are not always clear enough to permit a confident forecast of developments. Météo-France tries to give the maximum notice of dangerous developments at mesoscale and synoptic scale; unfortunately it is not yet possible to do this at the small scale (e.g. waterspouts), but happily these are rare.

The situation on 31 August to 1 September 1992

At 500 hPa (Fig. 1)

A broad trough lay over the west coast of Europe at 0000 UTC on the 31st with the greatest curvature and strongest flow NNW of Coruña. The vorticity maximum (Fig. 2) moved east very close to the Mediterranean coast at 0000 UTC on the 1st bringing a strong vorticity gradient between Corsica and the continent. Cold advection was strong over the continent but weak over Corsica. The geopotential and thermal troughs sharpened during the 31st, emphasizing their passage.

At 850 hPa (Fig. 3)

A deep low was centred north of Scotland at 0000 UTC on the 31st associated with a mass of cold air, with a temperature of 0 °C over Northern Ireland. The thermal and geopotential gradients were strongest near Spain. The trough sharpened and the geopotential gradient increased with the advection of cold air. The difference was marked with the warm air at 12–14 °C and the cold at 4–6 °C. The approach of the system strengthened the SW'ly current from Spain to the Mediterranean. The effect of the Alps was to create a low over the north of Italy (Po Valley) further increasing the WSW'ly flow over the north of the Mediterranean basin (see the chart for 0000 UTC on the 1st). The advection of cold air at low levels reached Corsica during the night of the 31st/1st with a temperature fall of 6 °C.

At the surface (Fig. 5)

The cold front marking the boundary of the air masses was active, the temperature contrast was obviously

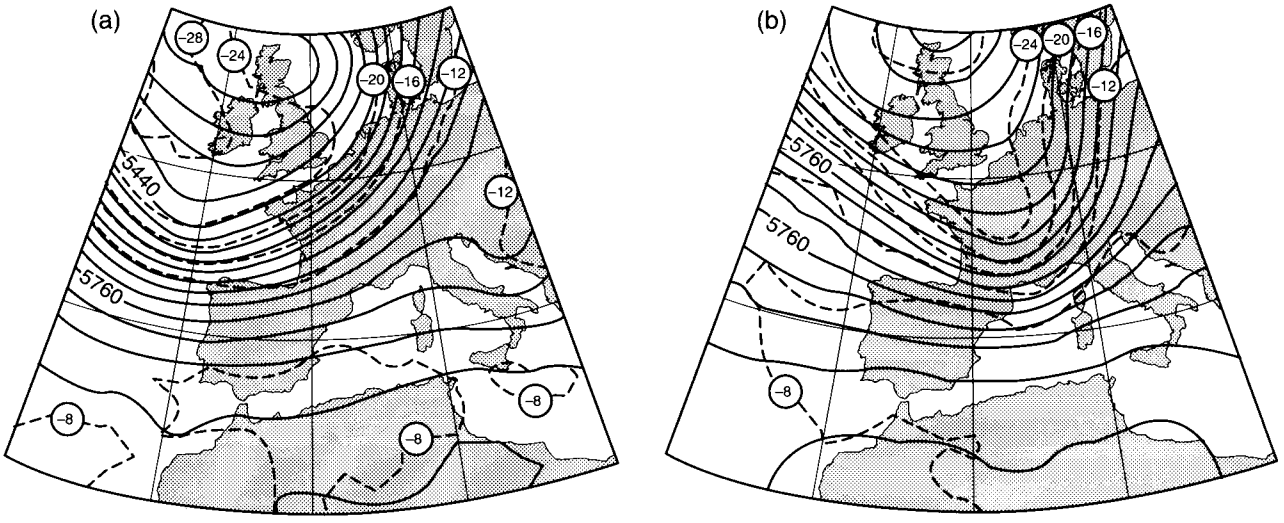

Figure 1. Charts of 500 hPa geopotential at intervals of 5 m and isotherms at intervals of 4 °C. (a) 31 August 1992 at 0000 UTC, (b) 1 September 1992 at 0000 UTC.

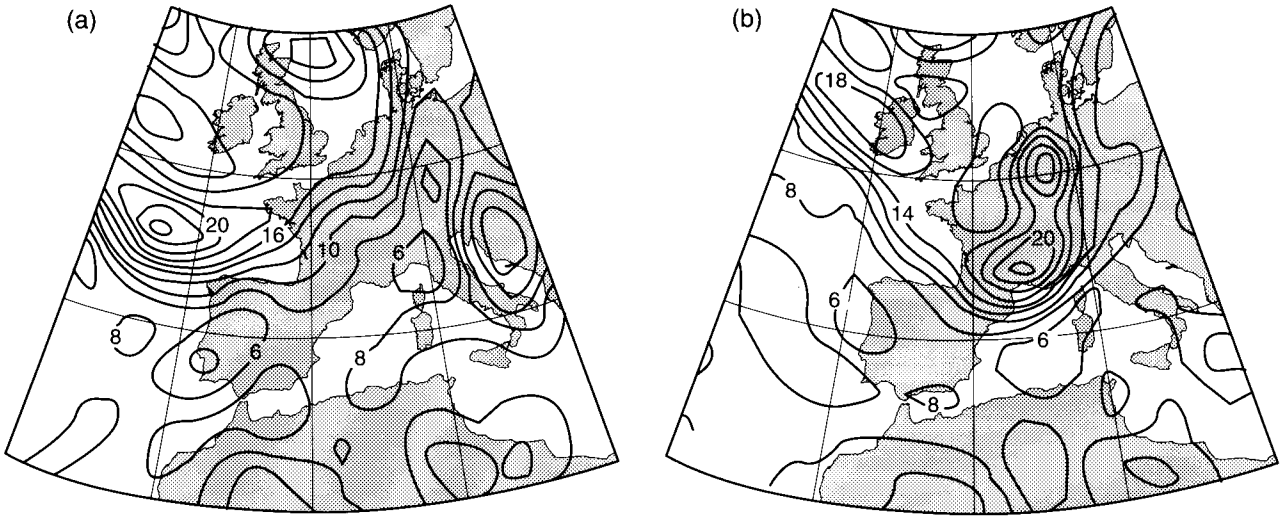

Figure 2. Charts absolute vorticity at 500 hPa at intervals of 10^{-4} s^{-1}. (a) 31 August 1992 at 0000 UTC, (b) 1 September 1992 at 0000 UTC.

important. Behind the front one can see strong subsidence on the 800 hPa vertical velocity chart (Fig. 4) for the 1st at 0000 UTC: it clearly marks the advection of cold air to low levels where it produced a well defined surface front.

Summary of these analyses

The burst of cold air, very marked at low levels, caused a significant strengthening of the gradient at all levels. This resulted in the acceleration of the low-level south-westerly flow. It was also accentuated by the creation of a dynamic trough to the east of the Alps. The strengthening of the south-westerly flow affected the whole of the western side of Corsica (see the observations at Calvi). After the passage of the cold front, the thermal wind at low levels and strong subsidence combined to strengthen the wind as it veered westerly. The northern part of the island was most strongly affected by this westerly flow (see the observations from L'Ile Rousse and Cap Corse). Despite the absence of marked cold advection at height, the passage of the cold front over Corsica produced the conditions for storm development. Essentially these are — a strong contrast in air temperature at low levels (see above) — the presence of warm sea at this season which increased the instability and supplied extra humidity — and cyclonic curvature at all levels associated with the geopotential gradient. (*Editor's comment: note also the abrupt change from weak warm advection to strong cold advection on the 850 hPa trough axis.*)

Remarks

This type of situation is classic in the Mediterranean towards the end of Summer and the beginning of Autumn when, in the absence of important cold advection aloft, low-level phenomena prevail. The

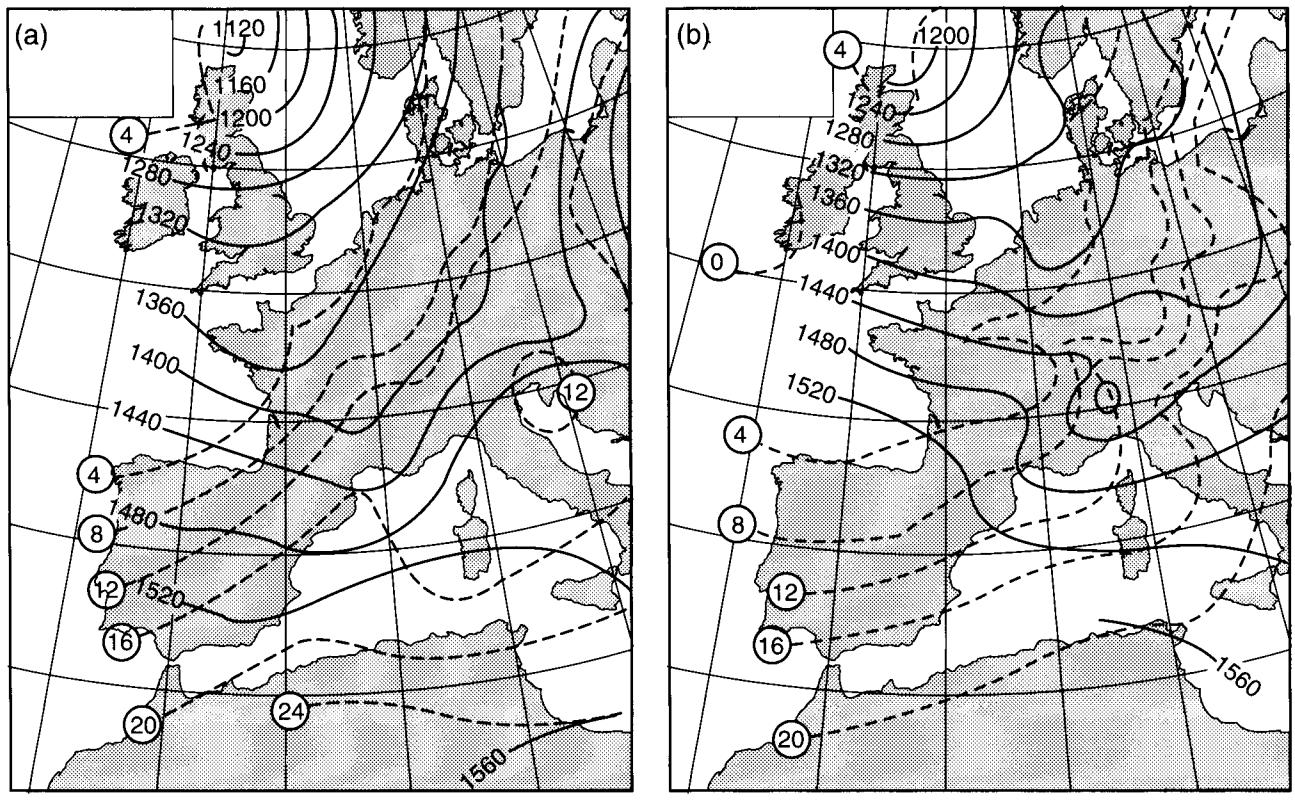

Figure 3. Charts for 850 hPa geopotential at intervals of 40 m and isotherms at intervals of 4 °C. (a) 31 August 1992 at 0000 UTC, (b) 1 September 1992 at 0000 UTC.

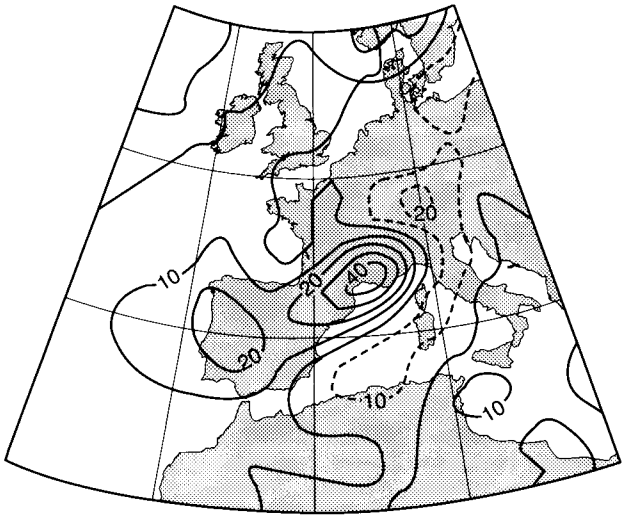

Figure 4. Vertical velocity at 800 hPa on 1 September 1992 at 0000 UTC.

absence of a strong thermal contrast aloft means the absence of thick cloud layers, except near the ground. There may be strong vertical developments with storms, violent at times, and accompanied by hail and very strong squalls. These storms can cause serious damage. Sometimes there will be cold advection aloft and this will be associated with a major reinforcement of the upper trough over the Mediterranean, leading to a marked increase in the intensity of phenomena, especially storm activity.

Study of the surface pressure field at mesoscale

A study of the pressure field at fine scale shows the local effects of relief on the wind flow. Corsica (Fig. 6) has a chain of mountains lined more or less north–south with many summits above 2000 m, the highest point, Monte Cinto, being at 2706 m. The maximum width of the island, east–west, is scarcely 80 km. The mountain chain plays a very important role in deflecting the flow of air at low levels, especially flows with a strong easterly or westerly component. In the present case the flow at low levels is well established from mainly the south-westerly direction, then veering westerly after the passage of a front. Fig. 7 shows local analyses of the pressure field at 2 hPa intervals both before the arrival of the cold air at low level (31st at 2100 UTC) and during (the 1st at 0300 UTC).

At 2100 UTC on 31 August

The formation of an orographic trough to the south-east of Corsica in the south-westerly flow is apparent; there is slack pressure gradient to the north and strong cyclonic flow south of Bastia. This cyclonic flow limits the increase in wind speed over the south-east of the island. The region around Bastia and the areas further north on the eastern side of the island are in an area of weak pressure gradient that produces a light wind. In contrast the gradient on the western side of the island is reinforced by the ridging over the south-west. Thus the south-west and north-west of the island are exposed to

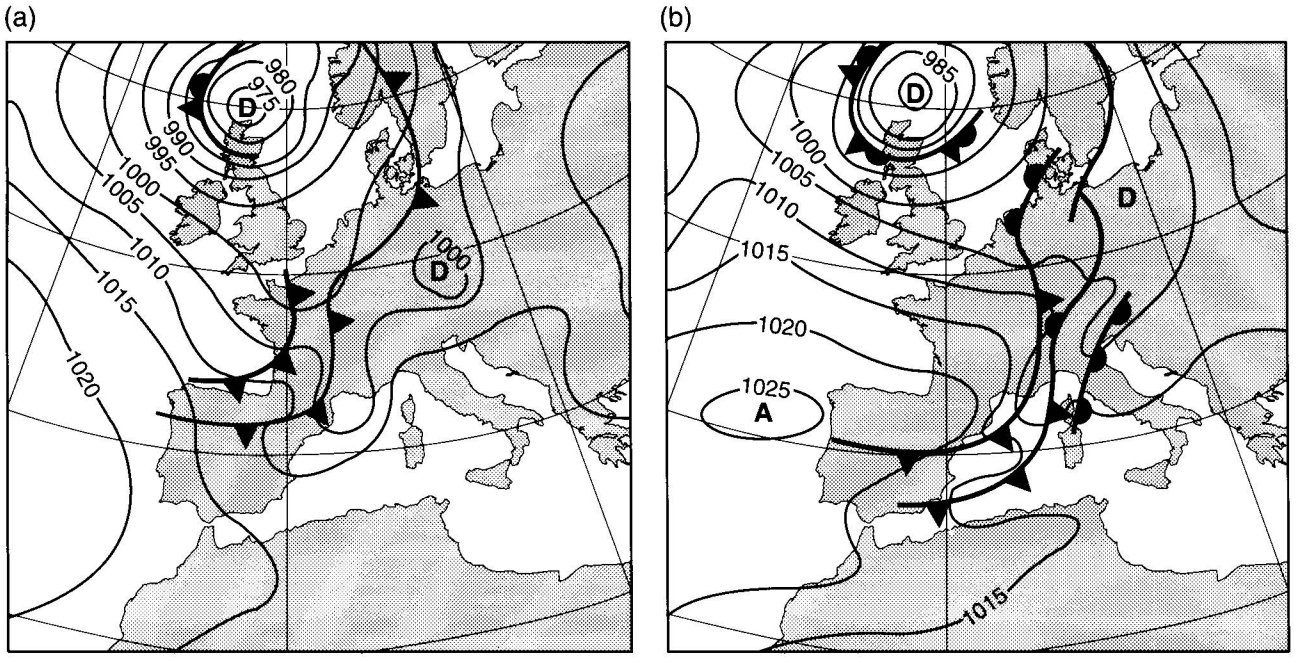

Figure 5. Surface analyses by Météo-France (with observations removed for greater clarity). Note that isobars are at intervals of 5 hPa: (a) 31 August 1992 at 0000 UTC, (b) 1 September 1992 at 0000 UTC.

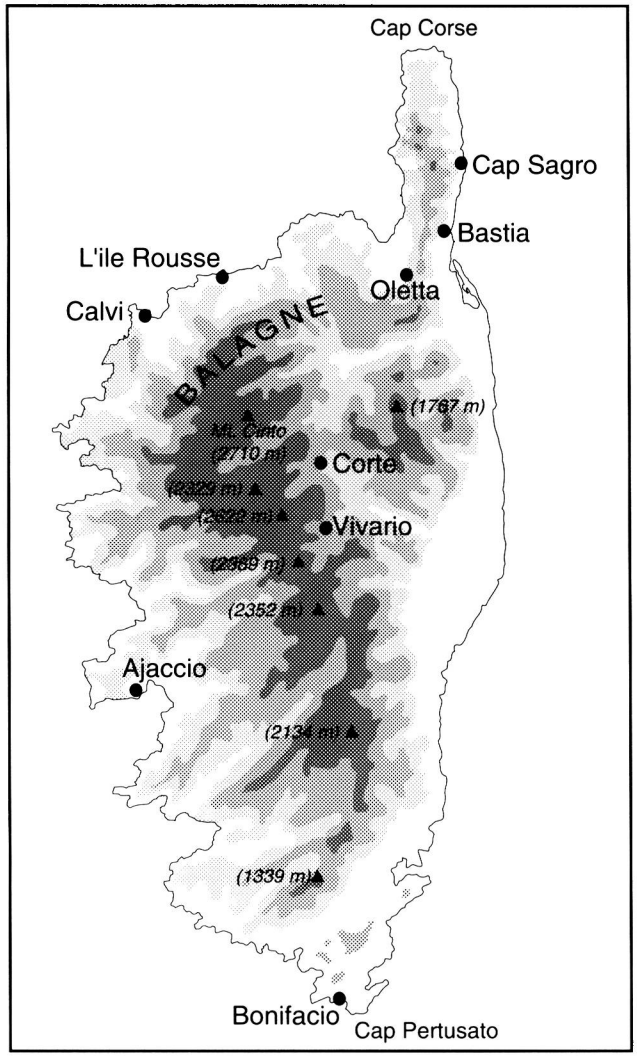

Figure 6. Sketch map of Corsica showing the locations of places mentioned in the text.

strong winds with a south-west component. The Gulf of Ajaccio is another favoured location for acceleration of the wind due to its orientation towards the south-west. The same is true at Cape Pertusato because of the funnelling through the Strait of Bonifacio between Corsica and Sardinia. The strongest winds were observed on the north-west of the island.

At 0100 UTC on 1 September

The cold air arrives. This leads to a rise in pressure, at least over the west of the island and the rise is most marked in the north-west where the pressure was lowest earlier. As well as a strong gradient the curvature has become more anticyclonic. With the turning of the gradient towards the west with the arrival of the cold air there is also a dynamic compression against the relief. The advection of cold air at low levels favours the strengthening wind and is accentuated by the curvature of the field anticyclonically. It is in this regime that we see the strongest winds. The dynamic minimum far south on the 2100 UTC chart tends to move towards the north. The most violent winds touch the north-west of the island around Cap Corse (26 m s^{-1}). We also observe strong winds in the extreme south of the island (Cape Pertusato); these are probably very local due to the configuration of the Strait of Bonifacio. The south-west of Corsica is subject to lighter winds (see Ajaccio).

The forecast

The strengthening of the wind was forecast by the services of Météo-France. A bulletin broadcast by the Centre Départmental de la Météorologie de Bastia (CDM Bastia) on 30 and 31 August is given below. The CDM at Toulon, responsible for general marine forecasts, broadcast special meteorological bulletins (BMS) to

Observations, Calvi — 31 August

Wind direction in degrees, true, speed in knots: cloud amount in oktas, height in feet

Time	Mean wind	Max	Cloud		
0900	200/11	29	1 Sc 4300	1 Ac 10 000	4 Ci 26 000
1000	240/20	33	1 Sc 4300	1 Ac 10 000	4 Ci 26 000
1100	230/17	33	1 Sc 4600	3 Ci 26 000	
1200	230/22	40	1 Sc 4600	1 Sc 6000	2 Ci 26 000
1300	230/17	35	1 Sc 4600	1 Sc 6000	5 Ci 26 000
1400	230/20	38	1 Sc 4600	1 Sc 6000	3 Ci 26 000
1500	230/22	40	1 Sc 4600	1 Sc 6000	
1600	SW/17–22 gusty		3 Sc 4600*		
1700	SW/17–22 gusty		5 Sc 4600*		
1725	230/29	42	Heavy rain shower*		

1800 to 2300 SW/17–22 gusty except around 2100 and 2300 when speeds were only 14 and 12 kn respectively. There were further showers and storms during the course of the night.

On 1 September the maximum 10-minute wind speed was 230° 29 kn at 0834 UTC. Maximum gust 200° 44 kn at 0321 UTC.

*Observed by the Editor.

Cap Corse		L'Ile-Rousse	
1200	060/06	1200	280/13
1500	080/04	1500	220/13
1800	280/06	1800	040/13
2100	260/15	2100	200/33
0000	280/49	0000	220/26
0300	260/58	0300	220/33
0600	280/62	0600	220/40
0900	280/49	0900	220/40
1200	280/40	1200	240/33

Summary of extreme winds (kn) on 1 September

Station	Highest mean	Highest gust
Cap Corse	280/73 0450	280/91 0510
Cap Sagro	280/49 0405	320/85 0945
Ile Rousse	220/51 0320	220/67 0350
Vivario	240/33 0130	280/62 0430
Corte	310/22 0130	280/44 0730
Oletta	250/24 0900#	240/42 1100#

in hour ending at

sailors and yachtsmen on 31 August at 0000 UTC and at 1200 UTC; this is given as well. These forecasts were made on the advice and consultation with the Centre Météorological Interregional de la Region Sud-Est (CMERSE) at Marignane (transferred to Bouches-du-Rhône, Aix-en-Provence, in January 1993) and the Service Central d'Exploitation de la Météorologie (SCEM) situated in Toulouse. The CDM of Bastia broadcast their forecast widely to the public by telephone answering services, broadcast bulletins to the media, press, TV, etc. and also to the security services (firefighters etc.).

Detailed weather forecasts issued by the Centre Bastia/Poretta

Night of Monday 31 August–Tuesday 1 September. Generally cloudy, becoming rainy during the course of the night. A more stormy spell is feared during the middle of the night. The storms may be violent but of short duration. They will be accompanied by hail, thunder and violent gusts. At the beginning of the night the wind will blow from the south-east in the east at 40–50 km h^{-1}, from the south-west in the west at 50–60 km h^{-1}. NB, a sudden, violent veer of the winds to the west is expected in the second half of the night. The zones most exposed in the first place are the Balagne and Cap Corse, and also cols and peaks in the interior.

Daytime Tuesday 1 September. Generally there will be little cloud but some instability cloud may develop inland over the peaks. The westerly wind will blow violently at around 70–90 km h^{-1}. with gusts perhaps reaching 130–140 km h^{-1}. The most exposed places will continue to be the west, Cap Corse, cols and peaks. Gusts are equally likely to sweep through the Bastia region and the mouths of certain valleys (Golo, Fiumalto, Tavignano, etc.). Maximum temperatures will be around 28–30°, in the east, due to the effect of föhn, they could rise to about 33–35°. The sea will be very rough in the west, rather rough to rough in the east.

Forecast for Wednesday 2 September. Continuing sunny. Winds becoming lighter, the winds will continue to be moderate over the west and Cap Corse to 50–60 km h^{-1} and gradually veer more north-westerly.

Forecast for Thursday 3 September. Hot and sunny. Wind mainly light to moderate NE. Maximum temperature 28–30°.

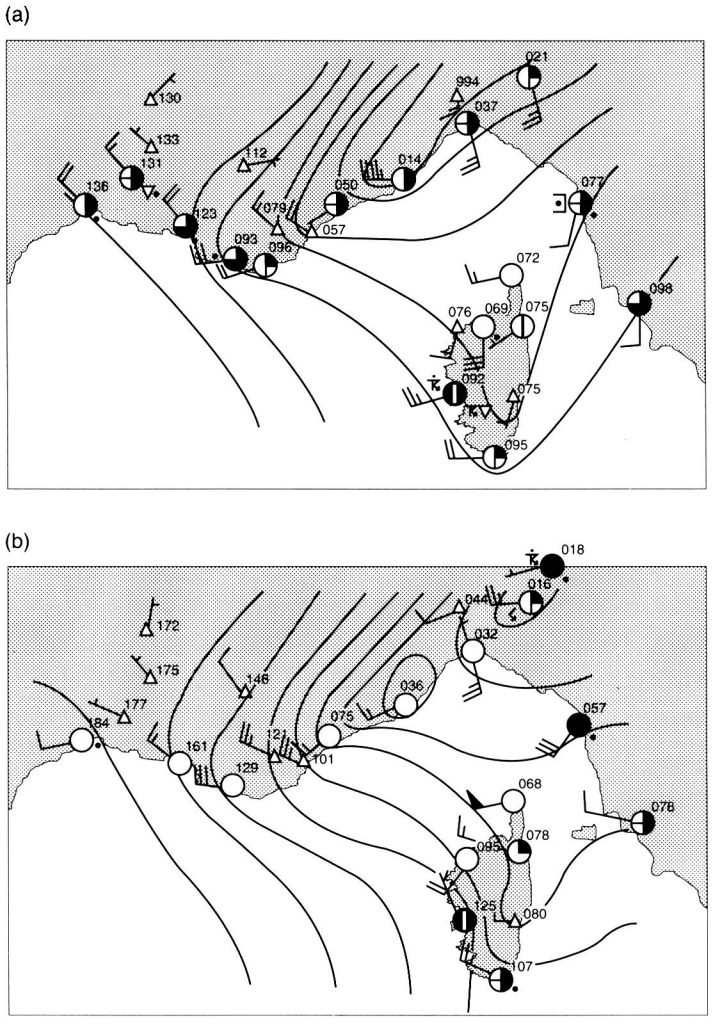

Figure 7. Simplified surface analyses using restricted plotted data with isobars at intervals of 2 hPa. (a) 31 August 1992 at 2100 UTC, (b) 1 September 1992 at 0300 UTC.

WHFX40 LFML 311200 COR
BMS MARINE DOMAINE DE LA COTE
ORIGINE METEO FRANCE TOULON NR 066
CE LUNDI 31 AOUT 1992 A 1300 UTC
DEBUT DE VALIDITE: LUNDI 31 AOUT 1992 A 1300 UTC.
FIN DE VALIDITE: MARDI IER SEPTEMBRE A 1300 UTC.

-ROUSSILLON LANGUEDOC:
VENT DE NORD-OUEST FRAICHISSANT FORCE 8 34/40 NOEUDS
LOCALEMENT FORCE 9 41/47 NOEUDS VERS BEAR.

-OUEST PROVENCE:
VENT DE SUD-EST FORCE 8 34/40 NOEUDS LOCALEMENT FORCE 9 41/47 NOEUDS.
VENT S'ORENTANT AU NORD-OUEST DANS LA SOIREE DU 31 AOUT.

-EST PROVENCE:
VENT DE SUD-EST ATTEIGNANT PAR ENDROITS FORCE 8 34/40 NOEUDS S'ORIENTANT OUEST DANS LA NUIT DU 31 AOUT AU IER SEPTEMBRE.

-OUEST CORSE LOCALEMENT EST CORSE:
VENT S'ORIENTANT OUEST A SUD-OUEST FORCE 8 34/40 NOEUDS DANS LA NUIT DU 31 AOUT AU IER SEPTEMBRE ET FRAICHISSANT LOCALEMENT FORCE 9 41/47 NOEUDS VERS BALAGNE ET CAP CORSE.=

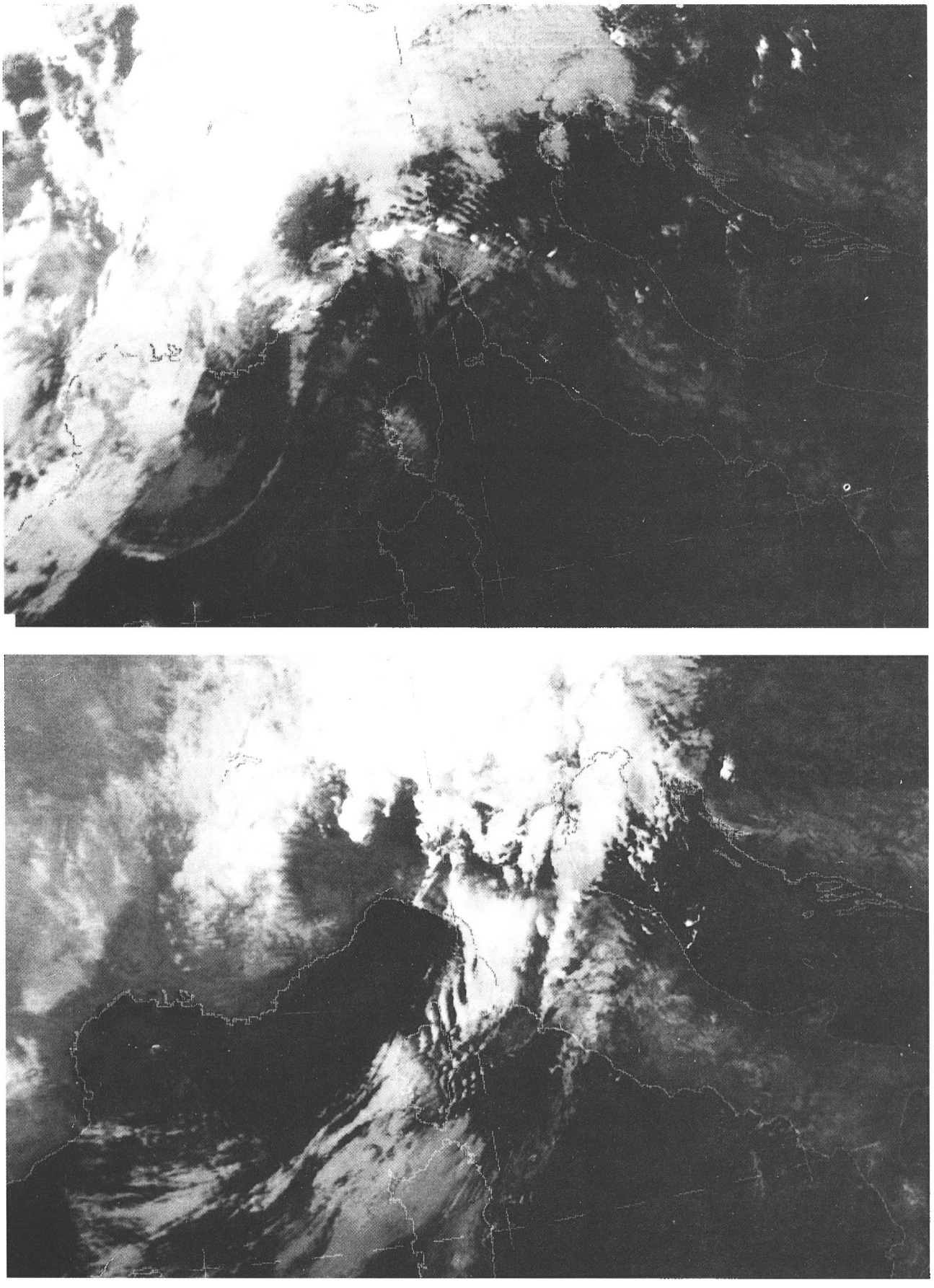

Figure 8. NOAA-11 IR images captured by Météo-France. Top, 31 August 1992 at 1745 showing cold air bursting into the Mediterranean basin. Bottom, 1 September 1992 at 0237 showing wave clouds downwind of Corsica and cumulonimbi over northern Italy.

Techniques used

The basic elements of the forecast are surface and upper-air synoptic charts and observations and forecasts. The output of the CEP (European) and ARPEGE (French) numerical models provide the main information about the medium-scale fields of humidity, the flow at various levels, absolute vorticity at 500 hPa (ARPEGE) and vertical velocities at 800 hPa (ARPEGE). The fields of vorticity and vertical motion are analyses and forecasts. We also have vital supplementary output for France from the fine-mesh model (PERIDOT) which is coupled to the ARPEGE model. These products are available in steps of six hours, up to 48 hours in advance.

Because of the broken relief this numerical model is best for the area and provides forecasts of precipitation, θ_w, wind and pressure at the surface, isotachs at 500 m, wind and temperature at 850 hPa, temperature at the surface and humidity at 700 hPa.

Low-level phenomena play an important role in the meteorology of the Mediterranean and we place much emphasis on the analysis and study of changes at low level especially those of wind (speed, convergence and divergence), vertical motion an θ_w. The most important information is available over the METEOTEL VDU system which is interactive. It provides charts and outputs from the PERIDOT model, satellite data (water vapour, infrared with cloud type and visible imagery), radar information both local and composite, sea temperature from high-resolution infrared satellite pictures and a display of lightning strikes updated every 15 minutes from the METEORAGE system. It is possible to run animations of images for satellite, radar and PERIDOT fields and to superimpose certain images; for example, a satellite picture and lightning, which is the best way of identifying probable storm cells. On the METEOTEL system it is possible to get the 700 hPa wind forecasts from PERIDOT and, using animation with the main cloud masses in satellite pictures to produce a forecast of cloud development. It is also possible to call up forecast cloudiness, certain vertical cross-sections and forecast radio soundings. METEOTEL is continually updated as new information become available.

A new version of METEOTEL, METEOTEL PC is being developed. It retains the features of the previous METEOTEL but has the advantage of a high capacity hard-disk store. This will permit animations of many more images as well as archiving a large number of fields. A fuller integration is envisaged with better imagery, summaries of observations and model forecast fields (the SYNERGIE system). Technical advances should permit zooming to a small area without loss of definition and the overlaying of fields of ones choice in different windows; all on a high-definition screen whereas the METEOTEL system has a simple TV monitor. In the new system too, updating of information will be continuous.

It should be noted that the south-east of France has a very dense network of automatic stations which allows events (mainly temperature, wind and precipitation) to be followed closely. They are an essential aid to forest-fire fighters and report several times a day, but may be interrogated at any time or continuously monitored (at one-hour intervals) if the situation requires it.

The development of the dissemination of forecasts

The 'forecaster's product' will change, thanks to the SYMPOSIUM system, in the long run the forecaster will only produce screen displays while many t .sks connected with the drafting of bulletins will disappear. The system will function in two steps, first it will load forecast information, and then automatically extract and display it according to the needs of the users outside Météo-France.

The forecasters' area will be divided into elementary zones of between a few hundred to a few thousand square kilometres and each will be treated as a single climatic region. The forecaster will load the database after each synoptic hour in the form of a chart for each parameter (or perhaps two or three), e.g. temperature, wind, cloudiness, precipitation. The value of a parameter is decided for each elementary area, and it is planned to use output from ARPEGE to initialize the database. The forecaster will then be able to control, or perhaps modify, the automatic forecast. This output can then be automatically be put into form of forecast wanted by the users (grids of data, frames of information; linguists are working at Météo-France on the automatic production of text).

Structure of the forecast service of Météo-France

The responsibility for analyses and their interpretation is pyramidal, the apex is the Service Central d'Exploitation de la Météorologie (SCEM), at Toulouse. Here at the hub of the information network, lies the computing centre permitting the most powerful techniques. SCEM provides the fundamental analyses at all levels, general advice for internal use at MétéoFrance on the evolution of fields and their interpretation, taking into account the divergences between forecasts from different models and the experience gained from their use.

SCEM has the responsibility to provide special national safety warnings of dangerous meteorological events, and provides 'ALARME' bulletins to the Sécurité Civile du Ministère de l'Interieur or special CMS bulletins to the media. In this sense, SCEM is the meteorological guardian on the national scale. There is also a supervisory and forecast role for some locations outside France; the provision of special bulletins for Atlantic shipping and protection of aviation to some international destinations such as the Caribbean and Africa. It also supports meteorological stations at

airfields with international western European traffic, providing TEMSI charts of winds and temperatures for various flight levels.

A new way of providing information to airlines is being developed; this is a microcomputer with VDU and printer, connecting an airline HQ to a database fed by SCEM (the AEROMET system). This allows the companies to get on demand the information they want in form of a conventional chart. The system complements the système Interrogations Réponses Aéronautiques (IRA) which for many years has allowed airlines to obtain TAF, METAR and SIGMET data using just a simple printer connected to our database via a computer terminal.

The CDM

At the bottom of the pyramid are the forecasters of the Centres Départementaux de la Météorologie (CDM). Their role is to be the interface between Météo-France and its customers (the public, businesses, authorities). They provide the forecasts tailored to the requirements of each. The work entails elaborating on a fine-mesh forecast for a restricted area, the same as or smaller than a département. To provide a forecast on this scale naturally relies on a prior study of synoptic fields, aided by the advisories from SCEM and from the Centre Régional (see below). The CDM forecaster does an analysis at small scale taking into account climatology, topography, forestry and water features to refine the forecast.

The CDM has a responsibility for the safety of its département corresponding to the national responsibility of Météo-France. Equally it assists with forecasts with forecasts for any coastal waters in its département.

The CMIR

In the middle of the pyramid, between the SCEM and the CDM, come the seven Centres Météorologiques Interrégionaux (CMIR). Their role is essentially that of an interface, partly technical between SCEM and the CDM (distributing technical advice affecting their region and monitoring synoptic developments) and partly between Météo-France and official organizations who want information or assistance at mesoscale (an area greater than a département) or at interregional scale. They are also the logical contact for the public utilities, the Centres de Coordination Interrégionaux de la Sécurité Civile, TV networks and regional radio services.

In addition, some CDM close at night, weekends and holidays and then their responsibilities are transferred to the CMIR.

Le CMIR for the Southeast Region covers 13 départements from the Spanish frontier to the Italian, the southern Alps, Corsica and the Cevennes.

Conclusion

This study has allowed us to show several aspects of Météo-France with an illustration of a particular meteorological event in the Mediterranean. It shows the essential — fundamental — role of the forecasters at CDM for the quality of the forecasts.

The local climatologies show strong contrasts across our region, from Corsica to the Alps, the Côte d'Azur to the Cevennes, the Pyrenees to Provence. The forecasters at the CDM are able to master the understanding of local effects of wind regimes, advection of air masses, etc. in way which regional forecasters, in charge of a much larger area, and even more the SCEM, cannot hope to match.

Acknowledgements

The author thanks his colleagues, Mme Roulle and Messieurs Rivrain, Bruno, Boussious and Rambaud for their help in preparing the paper. The editor thanks the European Centre for Medium-range Weather Forecasts for their corrections to his sometimes mistaken translations.

PS. As this article was being prepared for publication I received a copy of La Météorologie, *series 8, No. 6, June 1994. Its main paper is a case-study of torrential rain over Corsica in Autumn 1993. Although in French it should be easy enough to follow given some knowledge of that language and a dictionary. There will be another article in issue No. 7. — Ed.*

551.466.2

Modelling ocean waves

M.W. Holt
Meteorological Office, Bracknell

This is an edited transcript of a talk given at the Meteorological Office on 16 December 1992. A more formal and detailed paper describing the assimilation of ERS-1 data will be published in *Journal of Atmospheric and Oceanic Technology* Vol. 11, No. 5 (October 1994).

1. Introduction

I would like to start by acknowledging that although I am giving this talk there are actually three people involved in wave modelling in the Meteorological Office; Steve Foreman and Sophie Kelsall currently in Forecasting Research have had a hand in some of the work to presented. In earlier days Rachel Stratton and Rod Bromley and many other people also had quite a bit of input to some of the work actually presented here.

I thought I would start by putting into context where the wave model sits; the links we have with the other Divisions in different parts of the Office. During the course of the talk you will hopefully pick up how the wave model could be of use to the research side. On the other hand there are obvious commercial uses of the wave model output, so we will look at that later. I will start off with a review of recent progress in the wave model; in the middle section I will talk a bit about the instruments on ERS-1 of interest to the wave model, and the assimilation of satellite data (we have had over a year now to look at, and decide what to do with them). At the end I will present a short look at the idea of coupling the wave model to the atmosphere model, and getting feedback, particularly the surface stress over the ocean is wave-height dependent. And then finally some interesting plans where we think we might be going with the wave model over the next year or two.

2. Motivation

But before I get onto that I would like to give you some idea why we actually have a wave model, why we carry out wave modelling in the Met. Office and then a little idea of how a wave model actually works.

So why do we do wave modelling? Well there are really two main reasons; first is the research side and second it is commercially valuable, people actually want to buy forecasts, so we will have a look at that first. We forecast wave heights, the sea state and the wave period as well. In December 1991 a forecaster was out in the North Sea for some six weeks until a weather window could be forecast for a big job. Finally there came a spell with very low waves, but the operation was held up by swell of a particular resonant period for the lifting barge, so they could not actually do the work. Eventually a weather window was successfully forecast and the job was done. This shows it is not always the high waves that are important. Recently we have been providing the full forecast wave energy spectrum for similar operations. That is the offshore work, oil exploration, particularly in the North Sea, but it is becoming increasingly a global market. The Ship Routeing Bench in CFO looks after ships going all over the oceans, hoping to avoid the worst of the waves and so saving voyage time, and possible damage to the ship. Those two are the main commercial applications of the wave model output.

On the research side we see shall that the wave model is a very sensitive indicator of performance of the atmosphere models, I will be talking about the interaction of waves with the atmosphere. Of course the waves are at the air–sea interface, and there are obviously important details here for climate work where you need to get the fluxes of surface stress and various other quantities correct.

3. The model

So how does a numerical wave model work? First, we are not modelling individual waves. What we model is the wave energy spectrum, which is a statistical description of average sea state. If we think of the sea-state field at any particular time and place, we probably have a collection of waves of different frequencies, and travelling in different directions. Some will be swell, some will be wind–sea and directly related to the local wind. So we take that and represent the wave spectrum in terms of the energy level of the waves of a particular frequency, travelling in a particular direction. We come up with a polar plot like Fig. 1, for example, where wave frequency increases with radius. When we have represented the wave energy spectrum we evolve it according to Equation (1).

$$dE/dt + C_g.\Delta E = S_{in} + S_{diss} + S_{nl}. \qquad (1)$$

Equation (1) is the transfer equation for the evolution of the wave spectrum at each grid point. On the left-hand side we have the local rate of change and advection by the group velocity (that is frequency dependent — linear gravity waves are on the surface of the deep water, so group velocity depends on wave frequency). On the right-hand side we have various source terms. S_{in} is the

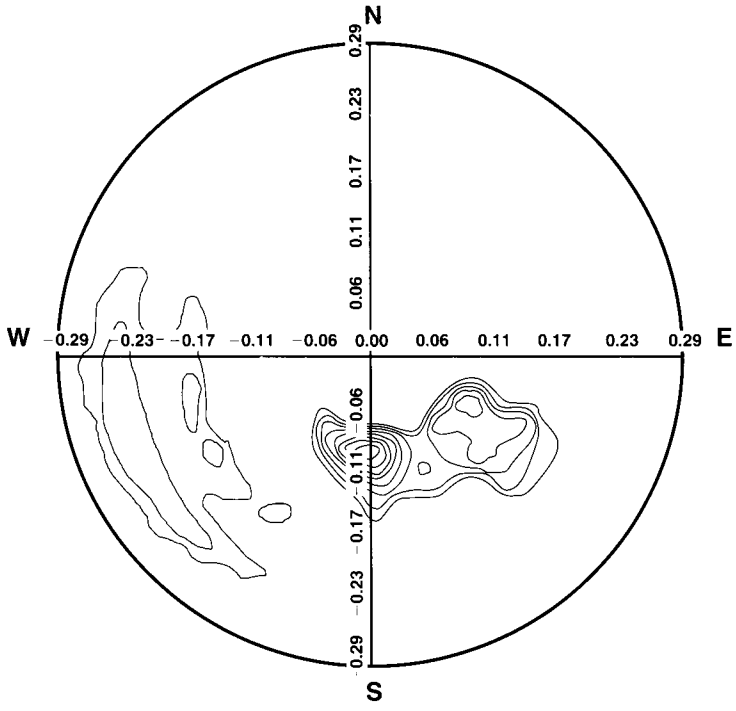

Figure 1. An example of a two-dimensional wave spectrum.

input term of energy from the wind stress to the waves; S_{diss} is the dissipation of wave energy, representing energy loss due to breaking waves and white-capping; S_{nl} is a non-linear transfer term which acts to represent wave to wave interactions and to transfer wave energy between waves of different frequencies.

Having decided what we want to do with the wave model we need to choose our wind data. As I mentioned earlier, it is very important to get the best possible wind data so we can make the best possible forecast of the waves: and we have a choice of using 10-metre winds, or the actual surface stress, or, as in our case, we use the winds from the lowest level of the atmosphere model.

Our global wave model has the same resolution as the atmosphere model and the grid coincides with the wind-data positions; we take the wind values hourly. These are considerations when you initially set up your wave model. You discretize the energy spectrum, and you have to choose the number of frequency components and choose how you want to allocate them; you have to choose the number of direction components as well. In our particular model we have 16 direction components giving an angular resolution of 22½°. The input term (S_{in}) is fairly standard, there is a common formulation used by most of the wave models in existence that is based on observations of waves. The dissipation term is a fairly standard formulation used in most of the wave models that are around and is based on an energy balance hypothesis. Where you can have a difference is in the treatment of the non-linear terms. This leads to the basic differences between one wave model and another. Our particular wave model, a so-called second generation model, parametrizes this term by forcing the growing wind–sea energy to take a particular spectral shape. We use a look up table, but it is a parametrization based on observations. As well as all that you have to choose your advection scheme and how you are going to do the time-stepping, and do you want deep or shallow water?

The next stage is to approximate these non-linear transfers and try to include some of the physics of what is actually going on. This approach is taken by the WAM (WAve Model) at the European Centre for Medium-range Weather Forecasts (ECMWF) and is called a third-generation model. The reason you have to approximate this is because the full calculation is extremely expensive in computer time, and has only been done for a single-point experimental model. The calculation can be done, but it is not practical to do so in a global model. The differences between the two simulations can become apparent particularly if you have rapidly turning wind; you can also continue the transfer of energy down to lower frequencies after the wind has fallen. The good news is that these effects, particularly the turning wind, are parametrized in our second generation model. The strategy that we have adopted for our research over the last two years or so has been, as far as we can, to concentrate on those aspects of the source terms of the formulation that are independent of whether your model is second or third generation and try to follow the work from there. At the same time we need to understand what differences there between these two approaches, because the question will come up soon when we have the computer power. Do we actually want to go towards the third-generation model, can we afford it? In the meantime we shall be using anything we discover to spin off improvements in our second-generation model.

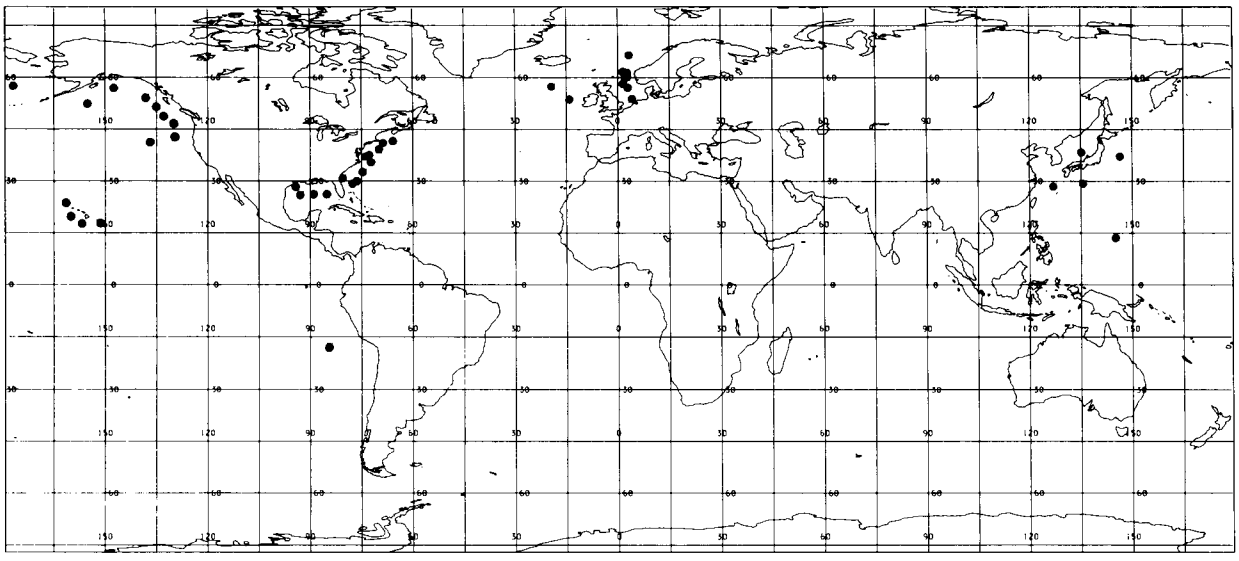

Figure 2. Locations of wave buoys and platforms.

Certainly there is a question facing us in the next couple of years, as to whether we continue with our current approach, or whether we take up the WAM.

In the global wave model we include a great circle propagation of swell. We take surface winds from the Global Model or indeed ECMWF model. The waves represented in our model range from the longest swell period of 25 seconds, which is a wavelength of almost 1 km, to the highest frequency, which is 3 seconds, waves which are 15 m long. In the Global Model, if we include coastal points as well, there are 37 322 data points on the grid and at each of these we have 13 frequencies and 16 directions. Operationally there is also the European model (which takes its wind from the Limited Area Model atmosphere) and covers the North Sea, the Mediterranean and the Continental Shelf areas; this version of the model includes shallow water effects. Before the ERS-1 satellite came along, we were not at all well off for observations. Fig. 2 shows there are a few moored buoys and many platforms in the North Sea, but there is only one buoy in the southern hemisphere. The majority are clustered on the continental shelf or close to it, and near to the USA. This has to be remembered when we look at verification figures.

4. Model intercomparison

We learned a few things from the intercomparison between our model and the ECMWF's WAM that led us to do some work to recalibrate our model. The trial was originally a four-way comparison, using Met. Office winds, ECMWF winds, our wave model and their wave model. We did it on the global grid at 3° resolution, which is what the ECMWF use. We used a direction resolution of 15° and when we did the verification we looked at the data from the model grid-point nearest to the buoy position. We ran the models for the month of November 1988, which happened to be a case already studied with detailed observations available. Initially we tried rescaling the different heights of the winds so that we ran the ECMWF model with our model's 10-metre winds and vice versa. We very quickly found out that that was not a good idea, instead we looked at runs of our model with our winds, and the ECMWF model with their winds. But the idea of the intercomparison was basically to have as much as possible in common, and for any differences to come from the model formulation rather than differences in resolution. Of course it is a further benefit to our model to be able to run at high resolution. Because of the formulation of the WAM, it actually has twice as many frequencies as ours because it has to physically resolve the transfer of wave energy. We looked at some verification figures and looked at the spectral output and all sorts of comparisons, and we eventually decided where some of the problems lay.

One of the things we found was that our model was lacking in swell in the Pacific and in the tropical areas. A time-series of wave heights from our model, WAM and one of the buoys in the central Pacific near Hawaii, showed that wave heights in both models were lower than the observed, but that our model is a bit lower than the WAM. There is also a diurnal variation in the observed wave heights and we have managed to represent this even if we do not get the height quite right; the evolution of the WAM is a lot smoother, probably because they use their winds at 6-hour intervals. We quickly found out that although the wave height was low where there was swell, it was not that bad when we also looked at cases in the north-west Atlantic. Off the coast of the USA there is a slightly different sea state regime; the conditions are dominated more by the developing depressions, and you have wave growth limited by fetch and by how long the wind is blowing, so you have far

more waves which will grow into equilibrium with the local winds. We find that under these conditions both models do fairly well; if the corresponding model of the atmosphere gets the storms right, then the wave model will get the waves right.

We also looked in detail at a case of turning winds and found that in fact the parametrization in our model was doing a good job, which was useful confirmation. The conclusions from the intercomparison were that behaviour in both models was fairly similar when it came to looking at wind–sea; in our model the parametrization of turning winds was effective, but we had difficulties and problems in the handling of swell. In the Pacific, the wave heights of both models were noticeably lower than observed. When we looked in detail at the spectrum, we found problems with an energy gap in the middle of the frequency range. Our model was lacking in energy there, but we were OK at the lower frequencies. This led to various changes being tested and we finally finished in September 1992 with a set of revisions. We changed the look-up table for the spectral shape (which is the non-linear transfer parametrization), we reduced the dissipation coefficient (which altered the energy balance at equilibrium) and we made a change to the section of code where we had identified we were losing swell in falling winds.

In Fig. 3 the symbols show you where our model frequencies actually lie. At one end is the energy from long waves of low frequency (that will be swell energy going in whatever direction); at the other end, of a higher frequency (that is shorter wavelength) are waves which are closely in equilibrium with the actual wind speeds. The figure summarizes the intercomparison showing what we did and what the WAM was doing at the same time. The solid line is the observed energy distribution and the line of short dashes (joining triangles) shows you what our previous model was doing before we amended it. They do not match well and the difference corresponds to 2–3 metres of wave height. The dotted line shows the energy from the final revised model and it shows that the revision has gone some way to reduce the bias, but there is still room for improvement. By comparison the dashed line shows the spectrum coming from the WAM — there is work to do with that as well. We looked at model verification at the buoy sites, we looked in detail at some of the spectra, but what was useful in retrospect was to look globally at where the improvement had come.

In terms of wave height, the difference between the revised model and our previous wave model shows a quite decent improvement in the model performance. This is particularly so in the central Pacific tropical areas where the revised model gives waves 60–80 cm higher than the previous one. The revised model became operational on 13 October 1992 and the verification taken one week either side of that data shows that we actually got the improvement we wanted, an increase of some 30 cm of wave height overall. However, that is not the whole story because we also have a time-series of Global Model verification going back to July 1987 and it shows (Fig. 4) a bias in the wave height. Bearing in mind that during this time there was no change in the Global Model but this was in the last days of the wave model on the Cyber before we introduced the Unified Model, you can see there is a reasonably steady downturn in the wave model performance over the years, even during the period when the model has not changed. During this time the model on the Cyber was unchanged but changes did take place in the atmosphere model. We find in particular that changes were made through the data assimilation scheme. The analysis correction scheme was introduced in 1988 and the wave model verification went down

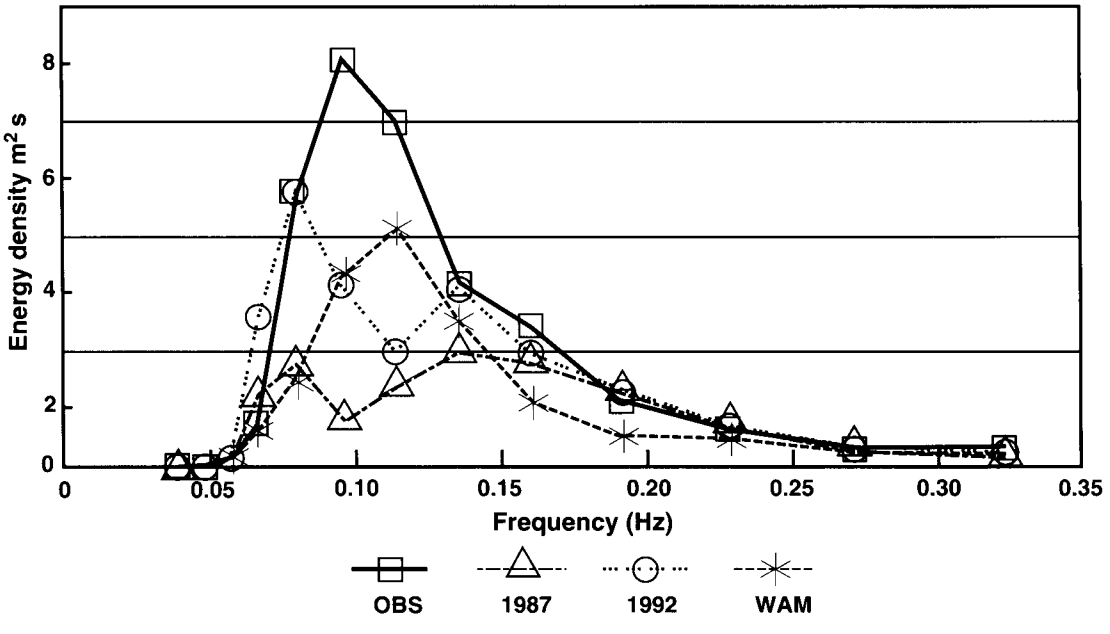

Figure 3. The distribution of energy in waves of various frequencies for the models.

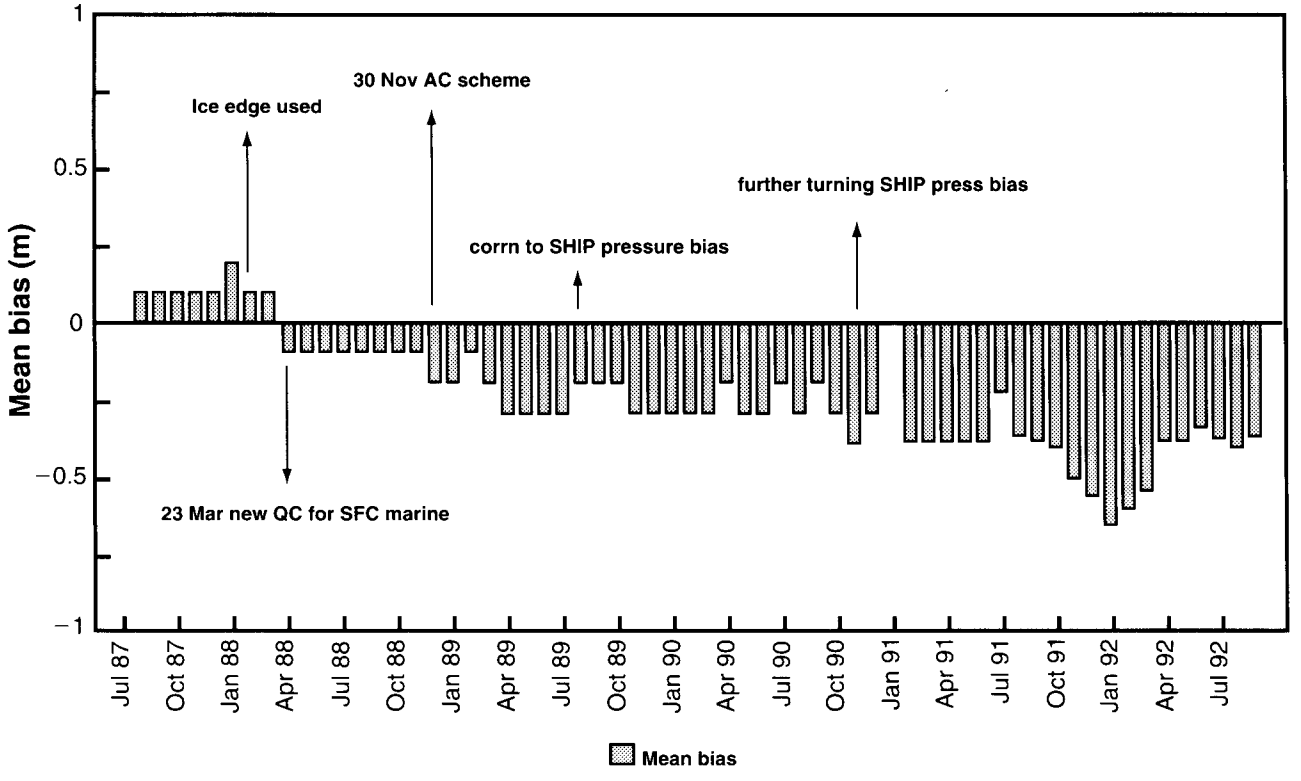

Figure 4. Changes in wave height bias in the Global Model Verification.

10 cm, due to a change in the ship observation pressure bias, and down again. So various things happened along the lines of data and changes in detail of the assimilation scheme. The wind speed verification actually looks good, verification of wind speeds against buoy stations shows a reduction in bias over the last four years, and we see the last few months match the observed very well. However, when you look more closely you realise that these wind speeds are from the lowest level of the model, at a nominal height of 25 m, and are compared with moored buoys with anemometers at a height of 5 m. We suspect that the wind speeds in the atmosphere model are a little lower than they ought to be at the surface.

Another thing we found in practice is that, because all these moored buoys have reported using SHIP code, the data is actually being put into the model at the height of 25 m. So we have learned that the performance of the wave model depends critically on the atmosphere model getting it right, and so hopefully operational changes, if they are likely to affect the surface wind speed, should consider the likely impact on the wave model, ideally before they are implemented.

5. Impact of satellite data

There are three instruments on the ERS-1 satellite directly of interest to wave modellers. The altimeter measures wave height and wind speed at the point directly below the satellite over the oceans. The scatterometer measures a swathe of surface winds which can be assimilated into the atmosphere model. The third instrument is the synthetic aperture radar (SAR), this can give you the full frequency and direction energy spectrum at any point where the measurement is made.

We can compare the location of the buoys in Fig. 2 with the typical 12-hour coverage from the altimeter shown in Fig. 5, and you can see that now we are covering quite a lot of the ocean surface during that time. So obviously it is useful, as most satellites are in that respect. A particular feature of the development of the calibration of the satellite instruments was the use of wave models and model data right from the start. A comparison of collocated model and satellite data quickly revealed some teething troubles with the satellite values, and these were soon corrected. It also showed that our model wave heights were lower than observed over much of the oceans and also that there will be spikes in the data which occur when the instrument is crossing from land to sea because it thinks it is very high waves — so obviously we shall have to quality control data before using it.

Apart from the fact that our model wave heights are a bit lower than observed, it led to the discovery of a calibration error in the software on board the instrument, that effectively meant the minimum wave height was 2 m. By comparing a large amount of model data collocated with satellite data, this was picked up fairly early on and the model data was extremely useful in correcting large errors in both (ERS derived) wave heights and wind speeds. ECMWF was also looking in detail at the wave-height data and I am pleased to say that the wave models were useful in finding rather more subtle errors in the formulation of the models. The scattergram (Fig. 6) shows the model wave-height of the

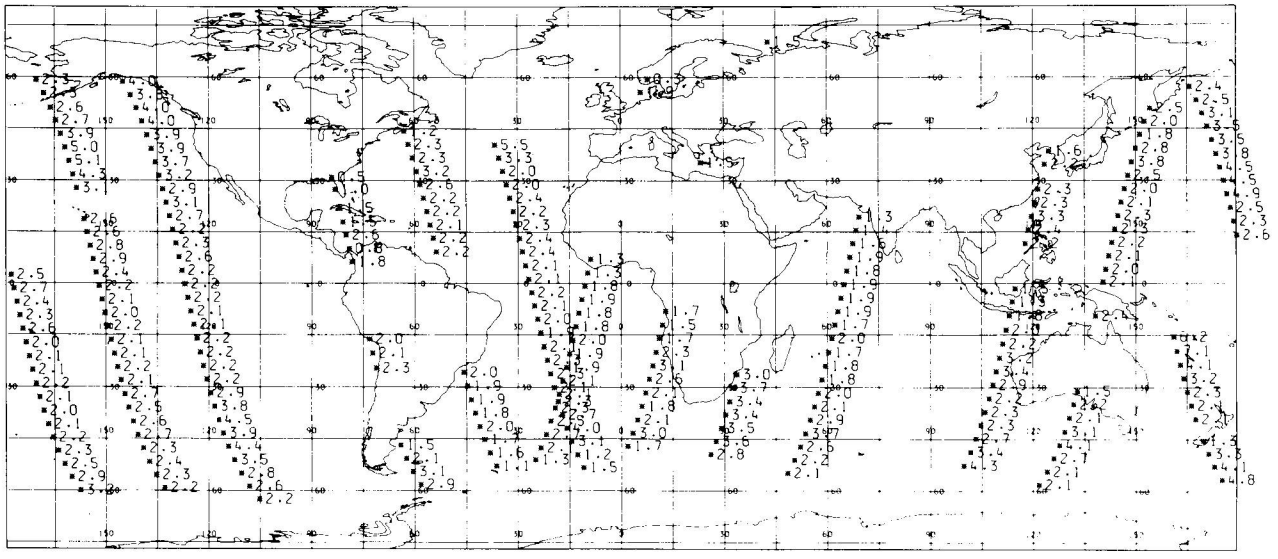

Figure 5. Typical 12-hour coverage of wave height data (m) from ERS-1.

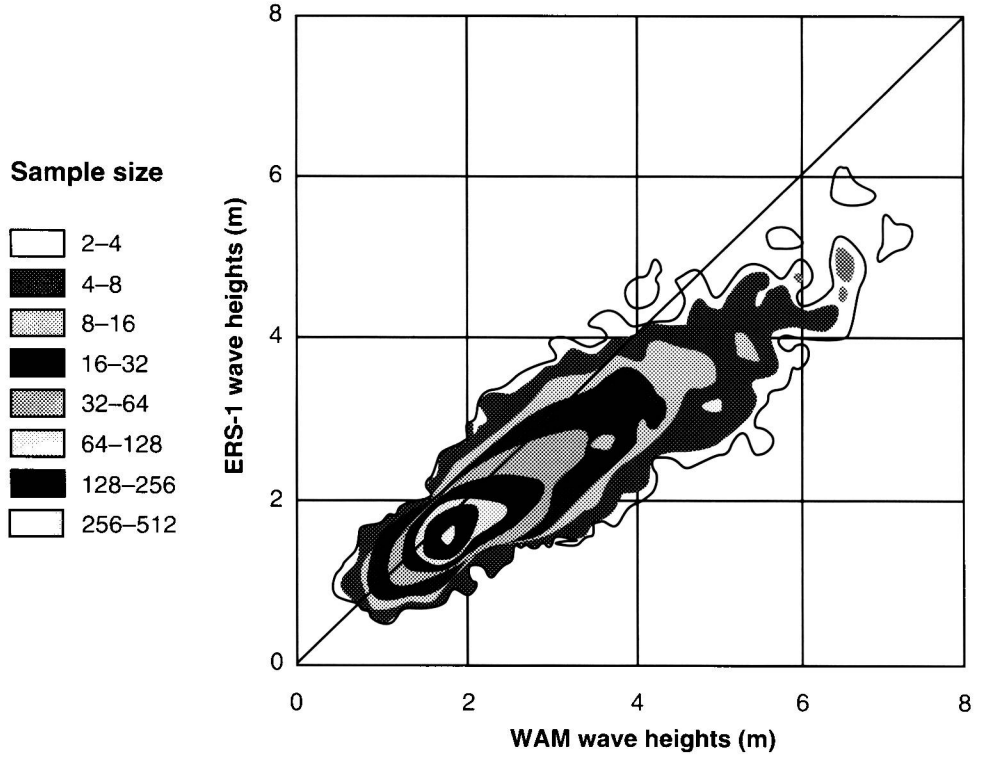

Figure 6. Scattergram of ECMWF WAM against ERS-1 wave heights for the period 6–13 October 1991.

ECMWF model against the altimeter wave height. When measured, the slope comes out to be 0.8, so they rang people at ESA who said "Of course, we have a 20% reduction in wave height, that was programmed in as a result of ground tests before take-off". That correction was soon taken out but it is difficult to see how this would have been discovered without comparison with the model data.

Having convinced ourselves that the information was useful we carried out a trial assimilation of the altimeter data of the wave height and the wind speed. The observations were processed in the normal way and spread out over an area that influenced some 300 km for the waves and some 200 km for the wind speed; so although the observation is purely at the point below the satellite, its effect is spread.

I will say a little bit now about the assimilation technique, it's magic, it really is, because we have two bits of information — wind speed and the wave height, and we go to 13 frequencies and 16 directions — 208 pieces of information — relying a great deal on what is already in the model. The basic principle is that we take the model wind speed and direction, and then split the wave energy at the point, into the swell part and the

wind–sea part. We have the observed wind speed so we can get an expression for the wind–sea energy (the amount of wave energy that is directly tied in with the wind speed). The observed wave height measured by the altimeter tells us what the total wave energy should be; so knowing the wind sea energy and the total energy, we can work out the swell energy that should be there after we have done the assimilation. That then defines the ratio of the swell before, to the swell after. The wind sea is set as it would be in the main wave model (you know what the energy level is so you use the look-up table) and rescale the model swell energy. We should end up — at the point of the model where we do the assimilation — with the model wind–sea energy matching the observed wind speed and the model wave height matching the observed wave height. You start with two pieces of information and end up with 208. That is how it works in principle. Actually its not as quite as easy as that, as there are some combinations of model swell and model winds that need to be correctly handled.

Now for some results of the assimilation trial we ran from the beginning of November 1991 to the end of January 1992. There was the odd gap when things occasionally 'fell over' or communications failed. The job was run twice daily as a 12-hour hindcast run, taking the winds from the operational model run that was current at that time. When we use Fig. 7(a) to compare the verification with the previous wave model we can see

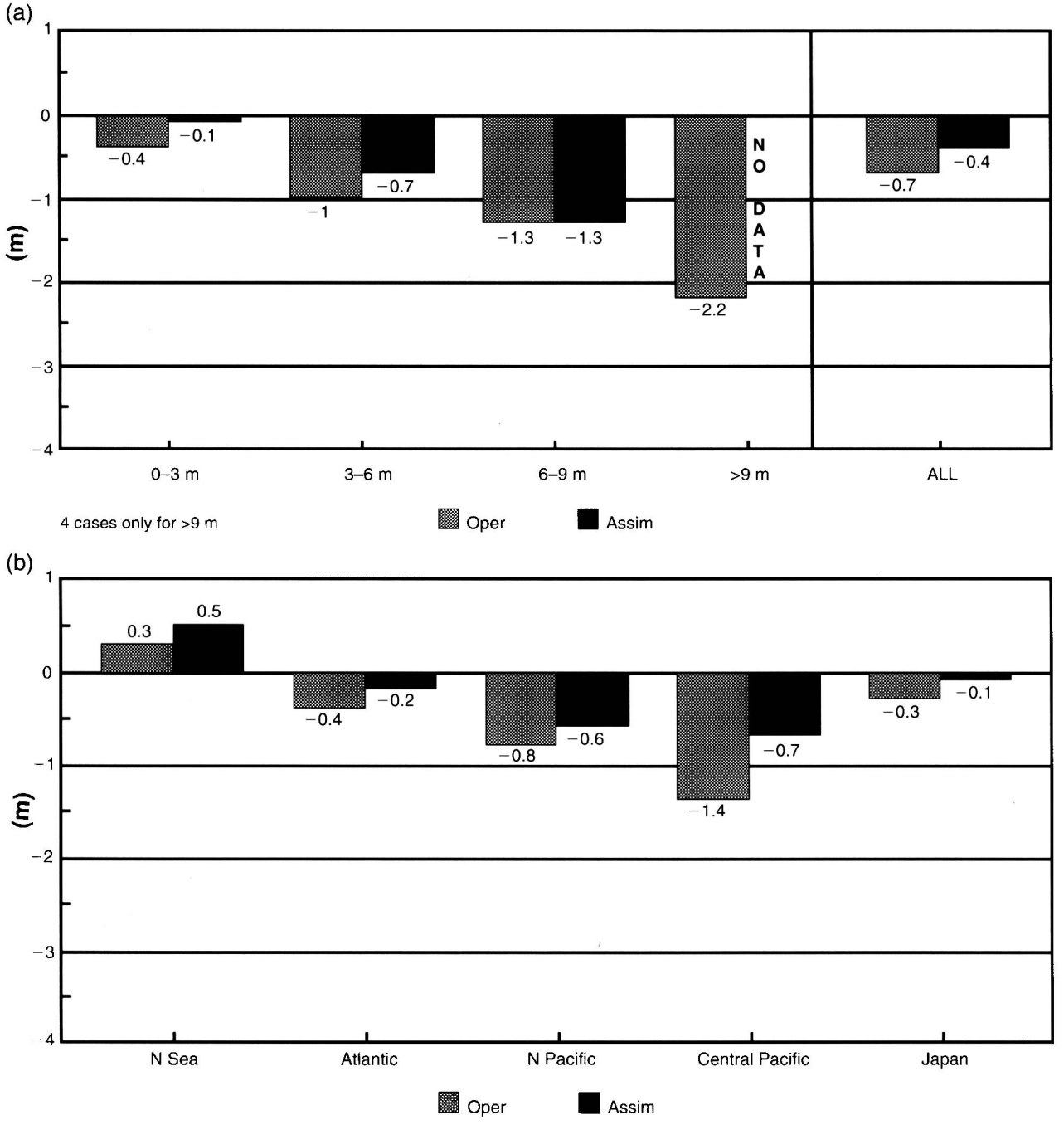

Figure 7. Comparison of verifications of the operational wave model run and with ERS-1 data assimilated (a) by wave height, and (b) by area

straight away how, for the lower ranges of wave height, we underestimate wave height in the model, and the impact of the assimilation is to bring the wave model back closer to where observed values would be, in fact by a mean of some 30 cm. If you break it down by region (Fig. 7(b)) the increases were larger than that in the tropics and central Pacific. Let us look at a time-series of all points in the Pacific. In Fig. 8 the dotted line is the observed, the dashed line is the current operational values for January 1992, and the solid line shows the run from the assimilation with the odd gap. It is obvious that the assimilation of the data has increased the wave height. We can see that when a satellite passes recently close by the information goes straight in; the wave height goes up — definitely some benefit from using the altimeter data correcting the model deficiencies in swell. If we look at one of the buoys off the east coast of the USA, because in the model the wind–sea is fairly well represented, the assimilation of the altimeter data has little effect. Occasionally we find that with because of an error in timing the swell will be increased there, but where the wave state is mostly dominated by wind-sea the assimilation has less effect.

If you look at a global map of the differences, you can see the separate satellite tracks that went in during a run and perhaps the run before, and large increases in model wave height underneath the satellite track. If you look at the difference in swell rather than total wave height you can see that the information about the swell in the sea gets spread out (an increase locally of up to 1 to 1.5 m). Information is retained and it is spread out between successive passes of the satellite. If we carry on with forecasting from the assimilated start field, we find the information in the swell is retained for two to three days into the forecast. When we rerun the assimilation trial with the revised wave model we would expect still to see an improvement in the swell height, remembering the revised model has reduced, but not entirely removed, the model bias in swell.

The second instrument was the scatterometer which measures a swathe of surface wind and here, thanks to Stuart Bell who ran the atmosphere model experiment, we did a six-day trial assimilation of the scatterometer wind in the atmosphere model, picking up the operational wave start field, and running it for six days with winds from the control run, and winds from the run using the scatterometer wind data. Looking at charts of wind speed difference at the end of that time we can see from the scatterometer data going into the atmosphere model there is really not a lot of impact. But occasionally there is, caused by the difference in position of a low centre; in one or two places you can see it actually moves the depression on. Looking at the wave height differences between the runs, again only small changes, in fact the global mean change in wave height was plus 1 cm, but there are local changes where at the end of this 6-day period the storms have changed position slightly, and this is in the northern hemisphere as well, not just confined to the southern hemisphere where we expected the greatest impact of the data. So less of an impact on waves through the atmosphere assimilation, but nevertheless a small increase in wave height.

The SAR is the third instrument, it is not straight forward to use. To get from the power spectrum as measured, back to the wave spectrum, you have to use a model's first guess spectrum. It is a non-linear inversion, and it is expensive (in computer time) and so for all these reasons, we at the Met. Office, have not been looking at data from the SAR. However, people at the Max Planck Institute, Hamburg, are working on it and developing algorithms for retrieving spectral data. So we hope to have SAR observations of the wave spectrum for model development eventually.

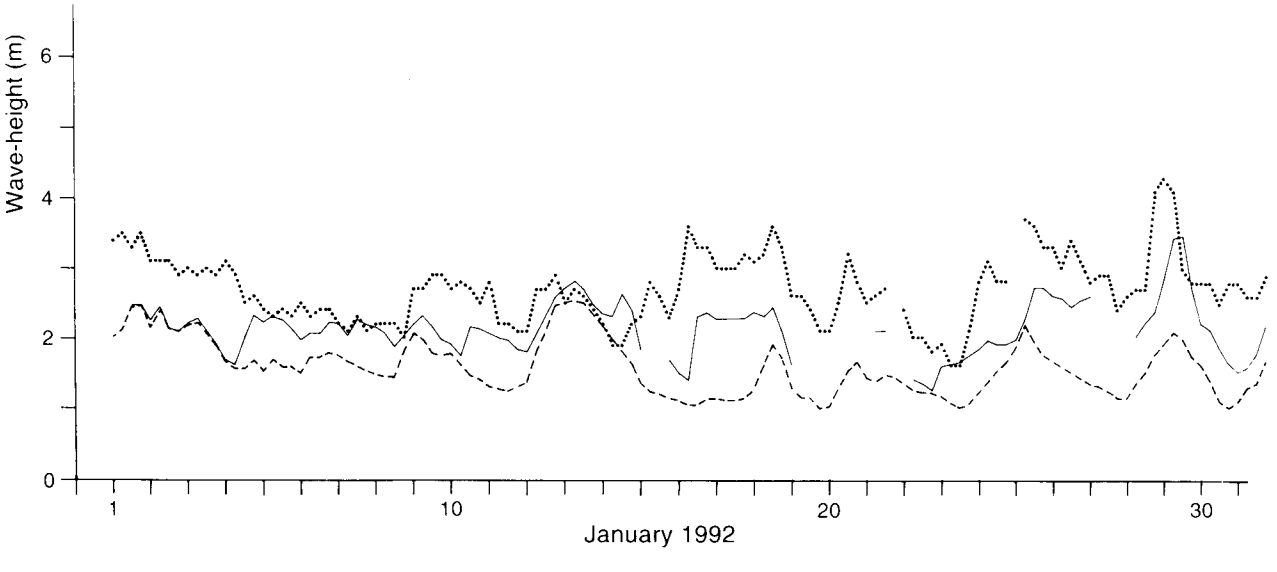

Figure 8. Time-series of wave heights near Hawaii; dotted line is observed, dashed line the operational forecast from the model then in use, the continuous line is the model run with assimilated data.

6. Wave–atmosphere coupling

I will now move on to some early looks at coupling the wave model to the atmosphere model. It is important to get boundary conditions correct in the atmosphere model, the correct surface stress and the correct drag. This is done by means of parametrization; you have to get the drag coefficient (C_D) right or, equivalently, the roughness length. Traditionally this is done in our Unified Model at the moment by the Charnock parametrization, which defines a roughness length depending on wind speed. Effectively the drag depends on wind speed only (remember the C_D is given by surface stress divided by the square of the 10-metre wind speed). There are various parametrizations from data sets of observations, usually in the form of a linear increase with wind speed. Now observations of C_D over the sea show that it can be greater than the mean value for the wind speed, if the wind has recently increased or changed direction. If the wind speeds have fallen then it is found that the C_D could be less than the mean value for the wind speed. Measurements over shallow water found the C_D was larger than expected, and measurements of growing waves under a sea breeze showed that the C_D actually decreases as the waves grow and then we reach a steady state. So there is clear evidence that the C_D depends on wave heights. The explanation is that in shallow water waves are steeper and present a rougher surface to the atmosphere. Now there are in fact very few observations of C_D over the sea for waves greater than 8 m or indeed wind speeds greater than 50 kn (for obvious reasons).

We can look at two particular expressions, one due to Large and Pond, familiar to climate modellers, and a more recent one by Blake incorporating wave height and wind speed (Fig. 9). Although it is still early days yet, I will show you some idea of the dependence on wave height, and how to calculate those two expressions for a particular wind speed and for growing waves from rest. Obviously the C_D depends upon wind speed, we can see there is more drag for small waves, and as the waves grow, the C_D decreases. You can see the Large and Pond data set has a fair mix of young growing waves and the mature waves, lying almost in the middle of the range of C_D given by Blake's expression. Now a look at how these things vary over the globe. The expression of Large and Pond, calculated on a particular day, shows a typical spatial variation of drag coefficient dependent on wind speed only. Comparing this with Blake's expression, the wave height dependence has reduced the C_D in areas of strongest wind. I might add that there are any number of different values quoted for the constant, so the reason I looked at the Large and Pond figures was because the measurements were over the open oceans, so it seems to make sense to use that.

7. The future

Now the longer term plan is, of course, to couple the wave model and the atmosphere model to get the stress right, probably by running the wave model and using the surface stress from the atmosphere model; we would then calculate the C_D or roughness length, including the wave information, and feed that back to the atmosphere model. However, within the Unified Model system that is not yet possible. There is quite a bit of effort needed with the internal diagnostics and the way information is passed between the models before we can do that. We cannot yet do the full coupling where the atmosphere gets the benefit of the wave information, but we can do the one-way coupling where the output from the wave model can be fed back to recalculate the surface stress that the atmosphere model is giving.

Work is also in hand with coupling waves to the Proudman Oceanographic Laboratory's tidal surge model. The point here is the coupling will include the wave–current interaction, you will have the varying

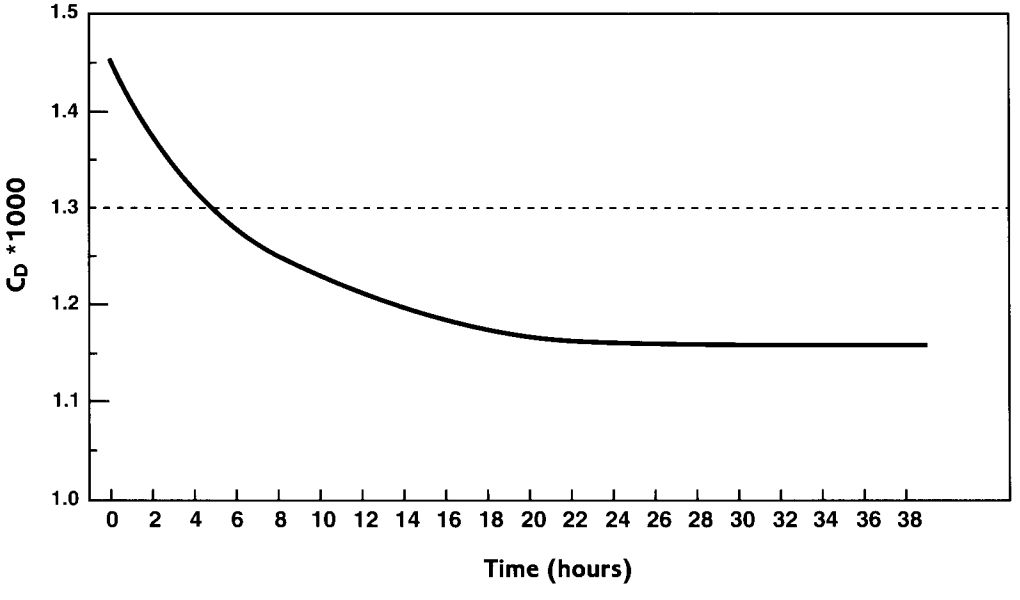

Figure 9. Two formulations of C_D for a wind speed of 15 m s^{-1}.

depth as well (at the moment the shallow water model does not use tidal variations of depth), so we could use those effects also to give a more realistic wave forecast.

We are looking at global shallow water (less than 200 m in this context), particularly at the request of Commercial Services Division because they want to open offshore markets in the South China Sea; and there is also the North Sea. The Global Model resolution may just be adequate to benefit from the inclusion of shallow water terms or maybe we will go ahead and develop a regional model. Then there is swell dissipation, nobody actually knows how much swell should be dissipated after it leaves the generation area and travels across the oceans; we certainly think we probably have too much dissipation of swell in the model. Finally we will look at possibility of assimilating altimeter data into the operational model. (Note: this assimilation became operational in June 1993.)

Editorial

Dear Reader,

This issue was prepared late in July 1994! That will explain why the magazine appeared to come to a premature end. I can only apologise for the long gap, caused by work on the Meteorological Office Annual Report and because much Editorial input was required for the two main articles. The paper on *Modelling Ocean Waves* had to be converted from a tape of a profusely illustrated talk, to something shorter while retaining the easy grammar that flows from the use of the first person. The paper on the *Corsican squall* had to be translated from the French into easy English; it was easy to understand when reading through quickly, but it was much more difficult to actually write down.

I ought to write a few words about recent Meteorological Office publications.

*The *Forecasters' Reference Book* sold so well when it was published in 1993 that stocks were rapidly exhausted. A further 1000 copies have been printed and are again available at £15 each (including handling).

The *Meteorological Office Annual Report 1993/94* is now available in three parts.
(i) **The Review* is a full colour popular account of developments in the period April 1993 to March 1994, and is available by post for £1 (to cover handling and postage); free on personal application.
(ii) *The Annual Report and Accounts* (ISBN 0 10 248394 9) is a legal requirement, is legal and financial, and probably not interesting to the majority of you. It costs £7.35 from HMSO.
(iii) **The Scientific and Technical Review* is in full colour for the first time this year and gives an interesting and, I hope, readable account of our research work. Copies are sent free to collaborators outside the Meteorological Office and to other Meteorological Services. However, if you do not fall into these categories, you may buy a copy for £5 (including handling) while stocks last.

The third edition of the *Handbook of Aviation Meteorology* (ISBN 0 11 400365 3) was published early this summer and is available from HMSO via good bookshops for about £30. It weighs 1.1 kg so postal charges may be important. It is so up-to-date that the Annex includes code changes introduced this year. It is essential reading for all aviators and so comprehensive, lacking in mathematics and well written by a team of experts, that I would strongly recommend it to all keen meteorologists who can afford it.

* To buy these send a sterling cheque made out to 'Public sub-account HMG 4712' to Publications, room 707a, Meteorological Office, London Road, Bracknell, Berks, RG12 2SZ.

551.576.11(410.11):551.515.127:551.557.2

Wave cloud

Figure 1 shows a fine set of Kelvin–Helmholtz billows taken by Mr. G.W. Oswin in Farnham, Surrey, England late in the afternoon of 7 December 1993. A powerful jet stream was approaching from the west and the core must have been close by at this time. The editorial staff saw the display from Bracknell but had no camera handy, and the official photographer was out on a job. It was with great joy that we learned that Mr. Oswin had taken the picture and sent it to the Enquiries Officer asking about the cloud formation.

As can be seen from Fig. 2(a), the horizontal shear ahead of the core was strong at around 45 kn per 60 nautical miles.

The hodograph of winds at Aberporth (A on Fig. 2(a)) is given as Fig. 2(b). The vertical shear between 500 and 400 hPa is 48 kn which in a standard atmosphere is about 10 kn per 1000 ft. The rules set down in the *Forecasters' Reference Book* suggest severe clear air turbulence should be forecast on both counts.

Figure 1. Kelvin–Helmholtz waves photographed about sunset on 7 December 1993 from Farnham, Surrey by G.W. Oswin.

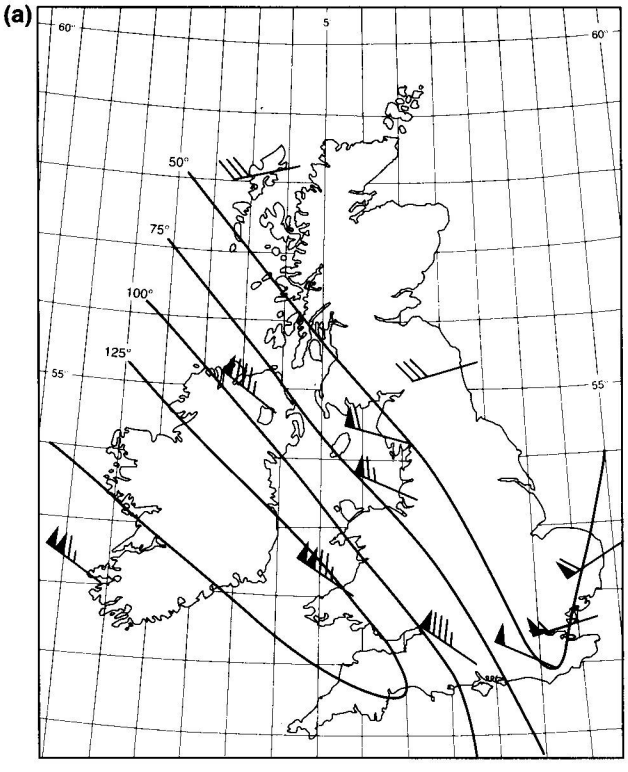

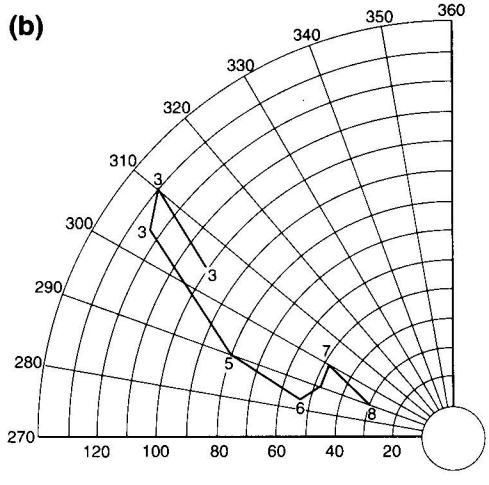

Figure 2. (a) Chart of 400 hPa winds over the British Isles at 1200 UTC on 7 December 1993. Isotachs are drawn at intervals of 25 kn. (b) Hodogram of winds reported by Aberporth at 1200 UTC on 7 December 1993. Small numbers refer to the pressure at each point in hundreds of hectopascals, speeds are in knots and angles in degrees true.

551.576.11:551.588.2.(49.1+491.2)

Orographic cirrus generated by Iceland and the Faeroe Islands — 4–6 May 1993

T.D. Hewson
Joint Centre for Mesoscale Meteorology, Reading

Summary

Fig. 1 provides two clear examples of orographically generated cirrus cloud, north-east of the Faeroes in 1(a) and north-east of Iceland in 1(b). Animated hourly images show the south-western edges of these cloud masses to be almost stationary, whilst filaments within the cirrus stream away to the north and north-east, wavering occasionally to the left or right. The appearance resembles that of a flame, or a flag being blown by the wind.

Insets in Fig. 1 show UK Met. Office limited area model (LAM) data for times close to those of the respective images. The south-westerly upper flow is broadly consistent with the location and behaviour of the cirrus.

It should be appreciated at the outset that most (if not all) theories and numerical simulations relating to orographic cirrus assume orographic barriers of infinite length. This brief study will relate cirrus features to individual peaks, and consider the effect of such peaks on downstream flow; in this respect the work is new. For this reason the results in sections 2, 3 and 5, which draw upon past work, must necessarily be treated with some caution.

1. Introduction

The cirrus to the lee of the Faeroes first appeared at 2030 UTC on 4 May 1993, and ceased developing around 1030 UTC on the 5th. Separate filaments of cirrus are labelled A, A′ and B on Fig. 1(a). Filaments A and B can be identified through most of the sequence. However A′ is transient; it originated some hours before in the position occupied at 0230 UTC by A, and then drifted eastwards, slowly decaying. The persistence of A and B suggests they can be related to topographical features of the Faeroes. The distance between the points of origin of A and B is very similar to that between the cluster of high peaks at the northern end of the Faeroes and the isolated 610 m peak at the southern end (Fig. 2), implying that the northern peaks probably gave rise to A and the southern 610 m peak to B.

The impression given by Fig. 1(a) that A and B diverge from their points of origin is slightly misleading. Images for other times shows their orientations to be similar.

Cirrus generation over Iceland began near the eastern edge of the island around 1030 UTC on the 5th and continued until 0630 UTC on the 6th. Filaments C, D and E were generally less persistent than those generated by the Faeroes — probably because of the complexities of Iceland's topography. Of the three D was the most persistent and C the least. Allowing for the fact that in Fig. 1 high cloud near Iceland appears about 40 km north-north-west of its true position*, it seems probable that the high-level glaciated region centred on 64.6° N, 17.2° W (Fig. 2) triggered D, and that the 2119 m peak triggered E.

*In overlaying a coastline on a geostationary satellite image it is generally assumed that cloud tops seen by the satellite lie directly above land features which would have been seen by the satellite had the cloud not been present. This procedure always positions cloud tops further away from the sub-satellite point than they actually are. Errors are usually small, but increase with both cloud height and distance from the sub-satellite point. At 0° W, 65° N, for example, cloud tops at a height of 10 km would appear about 34 km (or 0.3° latitude) north of their true position. Such errors are present in Fig. 1.

2. Waves at cirrus level

Orographic cirrus develops in the ascending branches of steady-state upper-tropospheric waves. These waves radiate well to the left and right of the region immediately downwind of the orography responsible for their generation. This explains (i) why on Fig. 1(a) the orientation of filaments need not be quite the same as the direction of the upper tropospheric wind (or 300 hPa height contours), and (ii) why on Fig. 1(b) the sharp cloud edge between 9° W and 14° W, and 65° N and 66° N (which was a semi-permanent feature) can also be attributed to Iceland's topography (see also Fig. 3).

Because vertically propagating orographic waves must tilt upstream with height (Durran 1986) waves in the upper troposphere typically begin some distance upwind of the triggering orography. Directly above this orography it is common for the air to be descending. This counter-intuitive result is supported by Fig. 1(b) — the dark band running from about 65.5° N, 18° W to 65° N, 15° W is due to cloud evaporation in a descending branch (referred to as a 'Foehn gap' in Reid (1975)).

A rough estimate of the upper tropospheric wavelength can be made on the basis of Fig. 1(b). Assuming that the coldest cloud in the cirrus filaments (at 65.9° N, 13.5° W) lies in a wave crest and that the warmest cloud just upstream (at 64.9° N, 15.2° W) lies in a wave trough gives a wavelength of about 260 km. This is not unreasonable given that wavelengths of vertically propagating waves should be much greater than the 4 to 40 km typical of trapped lee waves (which are responsible for the multiple cloud bands often seen in the middle and lower troposphere).

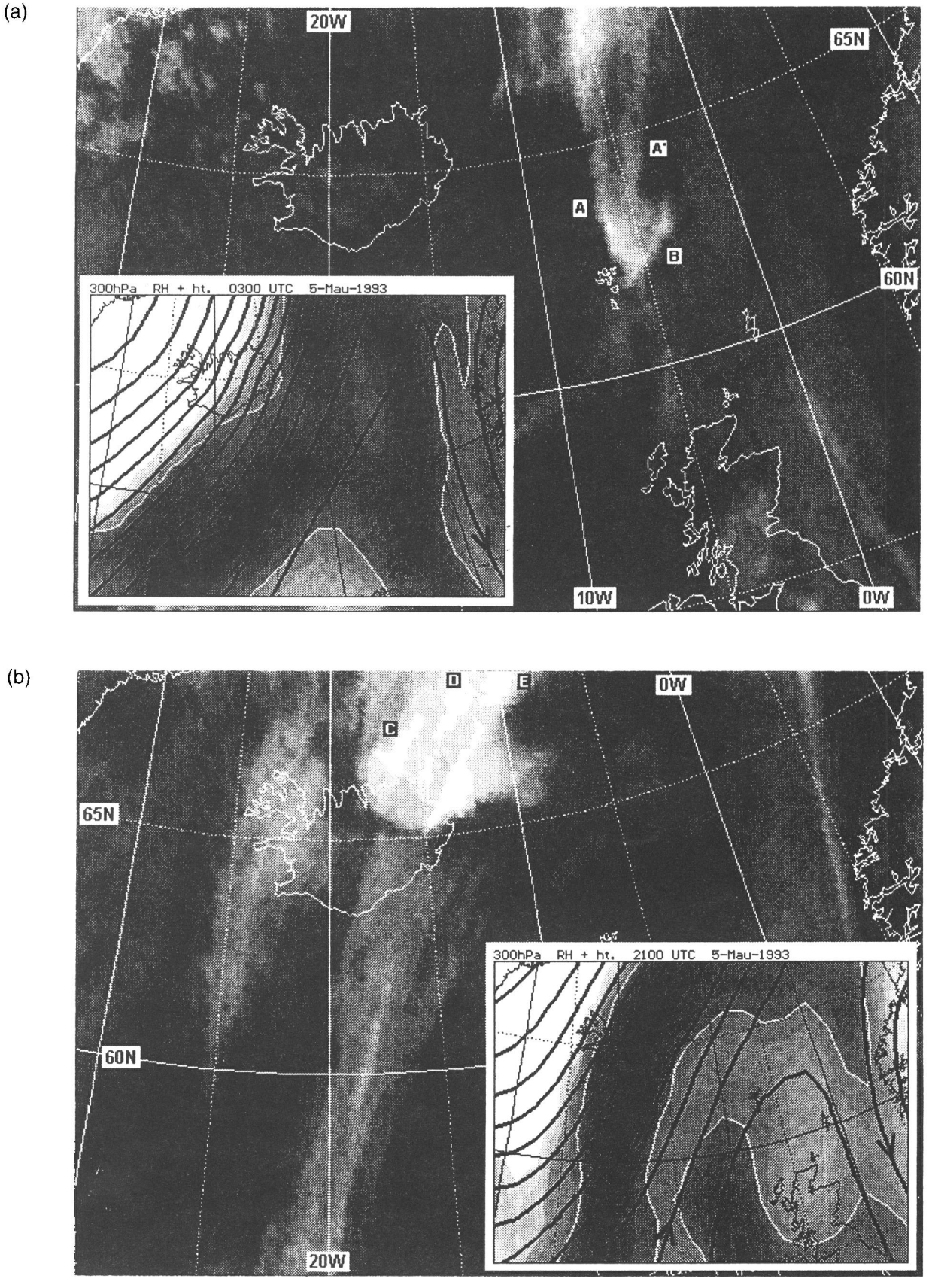

Figure 1. Meteosat infrared images for (a) 0230 UTC, and (b) 2230 UTC on 5 May 1993. Filaments of orographic cirrus are labelled A, A′, B, C, D and E. Insets show 3-hour forecast fields from the LAM for the 300 hPa level at 0300 UTC (a) and 2100 UTC (b) on 5 May 1993. Black contours are of geopotential height at 6 dam intervals. Shading indicates relative humidity with respect to liquid water. Darker shades indicate higher humidity, whilst white contours represent 60%. At temperatures of −50 °C at 300 hPa a 60% relative humidity with respect to water equates to about 100% relative humidity with respect to ice.

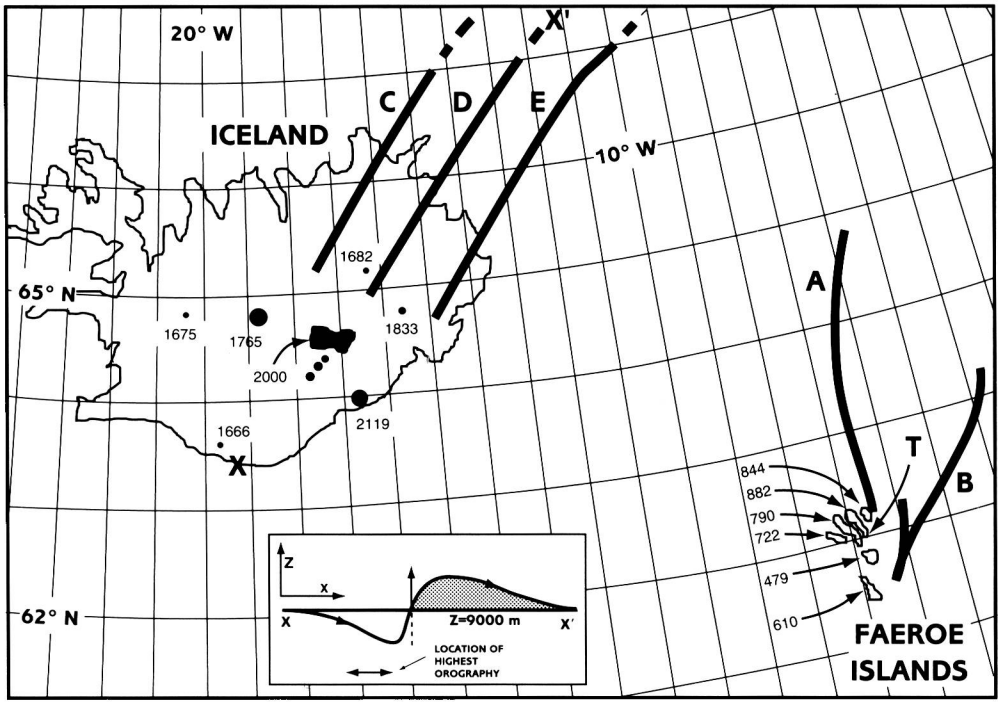

Figure 2. Topographical features of Iceland and the Faeroe islands. The major peaks in Iceland, and the high points on each of the six main Faeroe islands are labelled (heights in metres). Land/ice above 1600 m is blacked out. T marks the location of Thorshavn. Lines A, B, C, D and E represent the axes of the filaments marked on Fig. 1, having been corrected for the error noted in the footnote on page XX. The inset is a schematic representation, in a vertical plane, of a streamline through a steady-state upper-tropospheric wave (which gave rise to filament D on Fig. 1(b)). End points XX′ are marked on the main figure. Shading indicates the approximate location of the orographic cirrus. The small vertical arrow and dotted line are equivalent to those shown on Fig. 4.

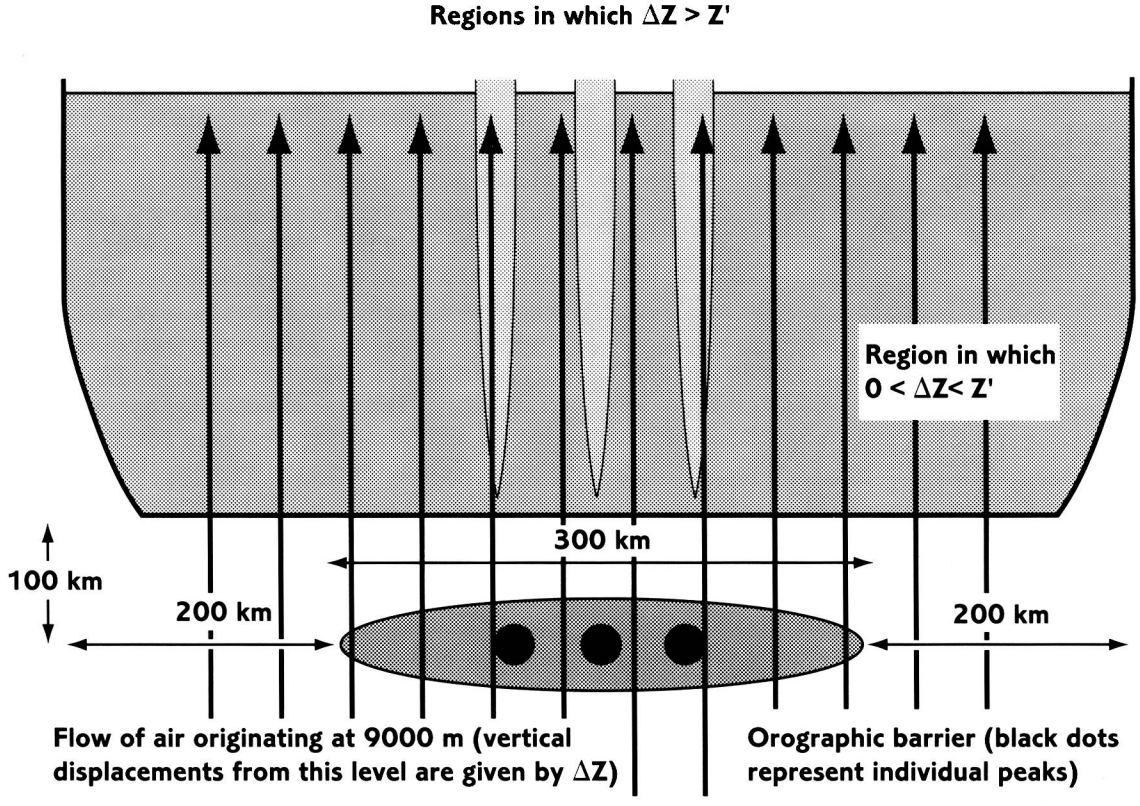

Figure 3. Schematic plan illustrating the regions (shaded grey and light grey) in which upper-tropospheric air can undergo positive vertical displacements as a result of flow across a finite orographic barrier (shaded dark grey). The diagram is based on observations in this case-study, and not on a numerical simulation of the problem. Approximate distances have been included. These are based on images of the orographic cirrus near Iceland.

In general there is only one wave trough and one wave crest. Downstream of the wave crest air descends relatively slowly, back to the level of zero displacement (see inset on Fig. 2). For this reason the cirrus' ice particles do not evaporate readily in the downstream direction.

3. Vertical motion at cirrus level

Cloud-top temperatures for the orographic cirrus were analysed using a sequence of hourly Meteosat infrared images. The minima attained in the lee of the Faeroes were −52 °C (in filament A) and −50 °C (in B). Downwind of Iceland the minimum (amongst C, D and E) was −57 °C. Comparison with the Thorshavn sounding for 0000 UTC on the 5th in Fig. 4 (assuming this is representative) suggests the coldest tops were just above the 300 hPa level, at heights of about 9900 m (A), 9600 m (B) and 10 600 m (C, D, E). These heights can be compared with those of the orographic features thought to be responsible for their generation, i.e. 900 m (A), 600 m (B) and 2100 m (C, D, E). The spread in the two data sets is similar, i.e. 1000 m (for the heights if the coldest tops) compared to 1500 m (for the heights of the orographic features). In addition the height differences between (A) and (B) are the same (300 m) in both. If it can be assumed that the orographically induced waves have the same level of zero displacement, and that there exists a relationship of the form

(Maximum wave amplitude) = k*(Orographic height)

(where k is peculiar to the atmospheric structure characteristic of this case study) then the similarities noted in the previous two sentences imply k is equal to or slightly less than 1. In other words the maximum amplitudes of the upper tropospheric waves which gave rise to the cirrus were probably similar to or a little less than the height of the orography below (enabling arrows and the level of zero displacement to be plotted on Fig. 4). Earlier observational work suggests such amplitudes are certainly plausible; in investigating cirrus generated by flow over hills in southern Britain, Ludlam (1952) concluded that hills 1000 ft high could cause vertical displacements of over 2000 ft at cirrus levels.

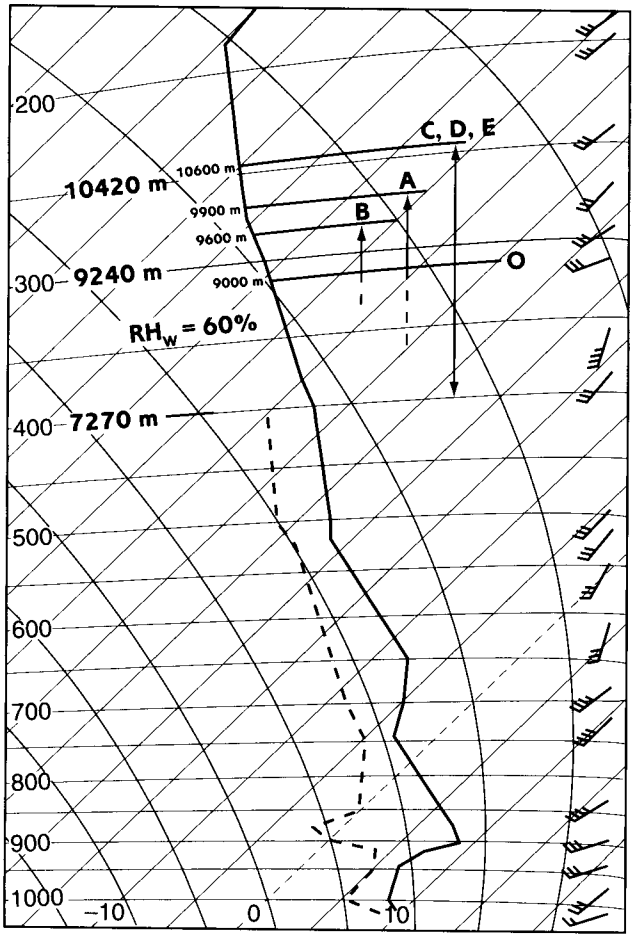

Figure 4. Tephigram for Thorshavn (see Fig. 2) for 0000 UTC on 5 May 1993. Winds are plotted conventionally, such that one full barb equals 10 knots. The geopotential heights of the 200, 250, 300 and 400 hPa levels are included. Heights shown for other levels have been interpolated from these values. Arrows give the maximum vertical displacements estimated to have occurred during the 4th, 5th and 6th in the ascending branches of the orographic waves which produced the cirrus filaments labelled in Fig. 1 (see text). The level of zero displacement is marked O. Dotted lines represent ascent between wave trough and level O (compare with inset in Fig. 2). A cross indicates the dew-point on the sounding (at level O) which would equate to a relative humidity with respect to water of 60%.

4. Thermodynamic aspects

Cirrus production requires ice supersaturation, i.e. a relative humidity with respect to ice (*RHi*) in excess of 100%. In the case of orographic cirrus this can be produced by forcing air with a RHi of about 100% to rise (and hence cool) within the ascending branch of the orographically induced waves. On the Thorshavn sounding the 300 hPa temperature is −47 °C; at such temperatures a relative humidity with respect to water (*RHw*) of about 60% will ensure saturation with respect to ice. The insets in Fig. 1 indicate 300 hPa *RHw* in both regions of orographic cirrus to be in excess of 60%. Indeed throughout 5th May orographic cirrus was generated exclusively where *RHw* was greater than 60% (LAM data). The time at which the drier air shown near 56° N, 15° W on Fig. 1(a) was advected across the Faeroes coincided exactly with the time at which orographic cirrus ceased to be generated there. Not only do these observations lend some support to the LAM's upper-tropospheric humidity analysis, they also suggest that LAM *RHw* fields could help in predicting orographic cirrus.

5. Vertical propagation of orographic waves

The generation of cirrus by flow over orography requires not only high humidity in the upper troposphere but also conditions which are conducive to the vertical propagation of orographically induced waves. In a two-dimensional mathematical representation these 'conditions' can be defined by four parameters; the width

of the orographic feature d, the wind speed U, a stability parameter N (the Brunt–Väisälä frequency), and the vertical derivative of the wind shear (see Durran (1986)). If the latter term is neglected (note that wind shears are small on Fig. 4) then vertical propagation will occur provided

$$3U/N < d \qquad \text{(SI units)*.} \qquad (1)$$

Substituting a typical value of N=0.015 s^{-1} gives

$U < 10d$ (with d in kilometres and U in knots).

So the propensity to generate orographic cirrus increases with increasing width of the orographic barrier. Narrower barriers generally require lower wind speeds. For $d \sim 7$ km (the approximate width of the southernmost Faeroe island in Fig. 2) U needs to be less than about 70 knots. Winds on the Thorshavn sounding are about 30 knots, so equation (1) appears to be satisfied.

Equation (1) also indicates that in general upward wave propagation is less likely if there is low stability ($N \to 0$); such as would be found in polar air masses over oceans, or during high insolation over land (see Ludlam (1952)). Conversely the marked inversion at 900 hPa on Fig. 4 (caused partly by prolonged advection across colder waters of air of tropical origin) would increase the chances of small orographic features, such as the Faeroes, being able to trigger orographic cirrus.

The magnitude of vertical displacements in the upper troposphere (and hence the propensity to produce orographic cirrus) depends partly on the amount of wave energy transported from below. This energy is larger if the wind speed at the level of the orography is larger. Thus the strong low-level winds over the Faeroes must also have aided cirrus production (given that they appeared not to have exceeded the upper limit imposed by equation (1)).

6. Implications for forecasting

The moist upper-tropospheric conditions required to produce orographic cirrus are frequently found in the vicinity of frontal zones, where jet-stream cirrus and cirrus generated by large-scale ascent are also common. For this reason the identification of orographic cirrus is usually more difficult than in the clear-cut example in Fig. 1. Nevertheless the benefits of positive identification are potentially quite high. Consider, for example, a case where high-level frontal cloud is cooling downwind of a range of hills. Realising that this is unlikely to be related to precipitation intensification would clearly be beneficial.

* To generate orographic waves Durran assumes a bell-shaped hill whose height h is defined by $h(x)=h_0 d^2/(d^2+x^2)$; where h_0 is the height of the hilltop, and d the horizontal distance from that hilltop to a point on the hillside where $h=0.5h_0$. In writing equation (1) it has been assumed that the 'width' of such a hill is approximately $3d$.

References

Durran, D.R., 1986: Mountain Waves. *In* Mesoscale Meteorology and Forecasting edited by P.S.Ray. Boston, American Meteorological Society.

Ludlam, F.H., 1952: Orographic cirrus clouds. *Q J R Meteorol Soc*, **78**, 554–562.

Reid, S.J., 1975: Long-wave orographic clouds seen from satellites. *Weather*, **30**, 117–123.

World weather news — July 1993

This is a monthly round-up of some of the more outstanding weather events the month, three preceding the cover month. If any of you, our readers, has first hand experience of any of the events mentioned below or its like (and survived!), I am sure all the other readers would be interested in the background to the event, how it was forecast and the local population warned.

South America

I know July is Winter down here, but it came as a surprise to learn that the Argentinian station at Maquinchao had a minimum of −23 °C on the 5th and Esquel a minimum of −13 °C. The Chilean capital Santiago nearly had a new record on the 12th when the temperature fell to −4.3 °C. Another cold day was the 25th when the Argentinian coastal town of Mar del Plata awoke to a temperature of −5.9 °C which was only 0.2 °C from the record for July.

North and Central America

On the 6th the west coast of Mexico battened down the hatches as hurricane *Calvin* approached from the Pacific heading towards Acapulco with winds of 85 kn and gusts near 105 kn. Much of the country was already suffering heavy rain from a tropical depression. By the 8th there were states of emergency in a broad band from Yucatan to Jalisco and more than 30 had died as a result of the incessant rain. Onshore winds did a lot of damage as well while the storm moved slowly north-west up the coast. One of the major causes for concern was a grounded chemical tanker with 4000 tons of sulphuric acid aboard: after the storm had passed the ship was reported to be empty and news of the environmental consequences was awaited. A weakening *Calvin* then

gave southern Baja California a taste of gales and heavy rain before dissipating over the ocean.

The major story has been the phenomenal rains over the Mid-Western states of the USA. which lead to catastrophic flooding over wide area astride the rivers Mississippi and Missouri. Nearly every day there were reports of record water levels and heavy rains (several centimetres). As with temperature references like 'twenty below', it is often difficult to tell what the datum is for quoted water levels. As the waters rose to cover locks the main channel became unusable for navigation and the massive barge trains stopped moving. Diverting the freight to the railways involved long diversions as many sections of track were under water and bridges in a dangerous state. On the 1st Lubbock, Texas, got its entire average July rain fall of 55 mm in one go: Bismarck, North Dakota, had 69 mm on the 2nd which was almost a record for July. Further north, Regina, Saskatchewan (Canada) had 91 mm between the 3rd and 5th (130% of the month's average). There was a further outbreak of heavy thunderstorms in the American Mid-West on the 7th which is said to have killed 15 and added to waterlogging problems (116 mm at Columbia, Missouri and baseball-size hail in Kansas with squalls over 50 kn.). The Mississippi finally burst its banks as it has threatened to do for some weeks; at St Louis its width was 7 miles. On the 9th parts of Iowa and Illinois had a further 70 mm (near record daily falls) and just after a flood crest had passed through Rock Island another 80 mm of rain fell overnight. On the 11th the levees around Des Moines were overtopped and the city's water processing works went under 3 m of water; Wichita's thunderstorm produced a gust of 88 kn and Princeton, Missouri collected 137 mm. By the 15th, with the Mississippi flowing at seven times the normal rate, sandbag-reinforced levees were giving way, spreading the floods, though reducing the level elsewhere. However, more rain was falling and the National Weather Service expected no major change for the next thirty days. The 16th saw the breaking of a levee which closed the last remaining highway bridge along a 200 mile section of river. Further thunderstorms added more water on the 18th, caused some more levees to fail and left 250 miles of the Mississippi without a usable bridge between Burlington, Iowa and Alton, Illinois. Upstream of St Louis there was a 300-mile uncrossable stretch until a bridge was reopened on the 19th. By the 20th the problems had spread further west as heavy rain overfilled dams and the Kansas River flooded.

A plateau seems to have been reached in flood levels by the 22nd but there were still some violent thunderstorms about with the threat of more widespread ones to come. The storms duly arrived over the weekend and the forecast date of the flood peak was put back until 3 August. Hamburg, Iowa, had more than 250 mm in the five days 21th–26th. Flood crests passing down the Missouri and Kansas were not in phase when they reached Kansas City on the 27th alleviating the threat of catastrophe. At the end of the month the city of St Louis was waiting behind its flood wall for the predicted 49 ft flood crest on August 2nd: the wall top is at 52 ft. By the end of the month estimates put the cost at 41 lives, $12bn and 16 000 square miles flooded.

Almost lost in the news of the floods came mention of a heatwave in the eastern states which had caused the deaths of 47. Temperatures over 30 °C in eastern Canada on the 10th were eclipsed on the 11th by an all-time high of 41 °C in New Jersey; more surprising was another new absolute record of 34 °C at Umiat, Alaska on the 15th. Towards the end of the month the northern states of Ohio and Pennsylvania were struck by storm of hail and wind, nearing 90 kn, that did nearly $45m of damage.

Australasia

This information is based on that kindly given by the Australian Bureau of Meteorology.

The 7th was a notably wet and windy day in South Australia and Victoria. Parts of south-west Victoria had storm force easterlies which closed the port of Portland for the day and mean speeds of 40–45 kn were quite common: the wind did more than A$1m damage around Adelaide. The heavy rain, around 60 mm over a large area, broke century-old records for daily rainfall: one of the biggest changes was at Murray Bridge in South Australia where the 107-year record changes from 23 to 37 mm. In the monthly total stakes there were many contenders for the prize, but at Temora the 113-year data set had 1891 as the wettest July with 130.2 mm; the record there is now 158 mm. In the prelude to this storm the wet 6th was especially cold at Broken Hill, New South Wales (NSW), where the maximum of 6 °C was the lowest for any month since at least 1948. In contrast much of NSW and Queensland had their warmest July on record; the mean minimum was a record high in many places and the mean maximum was also a record high in some.

The month ended with wild weather at two extremes; around Perth on the 29th many coastal sites recorded gusts of over 50 kn accompanied by thunderstorms: the next day damaging northerly winds struck Melbourne with 61 kn reached in gusts at the Dunns Hill AWS.

Asia

Heavy rain that started at the end of June over Zhejiang Province of eastern China continued into July leading to the deaths of six people by the 5th. Next day Hunan Province (central China) reported that their death toll had reached 33; further north there were fears that the Yellow River might burst its banks. In contrast Sichuan and west Hunan were suffering severe drought. The 13th brought news that the death toll from flooding in southern China was rapidly rising towards 100 after several days of heavy rain, especially in the province of Jianxi where, despite the efforts of a million workers, the town of Wuzhou was buried under the deepest floods in its history. Korea could hardly expect to escape the fate

of south China, and accordingly 'a wet front' dumped lots of rain over the south starting on the 11th; Seoul had over 170 mm, but Chonju, 125 miles further south had 250 mm. Six died and more rain was forecast. The north Chinese province of Shanxi took its turn to be flooded mid-month when seven were said to have been killed by the heavy rains. Train services were suspended (almost literally) on the 20th between Lanzhou and Urumqi in the extreme north-west of China after heavy rain caused flooding and washed away ten long sections of track; about 18 000 were caught on trapped trains. The last three or four days of the month brought further devastating rainstorms to Hunan and Sichuan Provinces — one report wrote of 530 mm in 21 hours near Emei City; not surprisingly there were floods and landslides which killed at least nearly 200 stranded thousands and washed away a freight train.

Tropical storm *Lewis*, born in the Philippines earlier in the month, affected Vietnam on the 12th then Laos and Thailand leaving a trail of flooding in his wake, but the death toll seems to have been small. Extraordinary rainfall of 315 mm in 15 hours at the southern end of the Japanese island of Kyushu caused havoc with at least seven killed by landslides, some of which were lahars from the volcano Mt. Ontake. In the last few days of the month heavy rain over Japan lead to flooding and landslides that killed seven people. According to a spokesman for the Japan Meteorological Agency, Kagoshima in the south of Kyushu had ten times the rainfall in St. Louis (USA) during this month.

On the 26th an Asiana Airlines Boeing 737 crashed in foul weather near Mokpo in the south-west of Korea on a flight from Seoul. Apparently it made some failed approaches before crashing into a hill 50 km away in driving rain: 42 of the 106 aboard a reported to have survived. Heavy rain in the Philippines caused some flooding in Manila on the 29th. The three-day downpour triggered lahars down Mount Pinatubo which in turn caused some secondary explosions.

Indian subcontinent

As I expect all our readers know, the dominating story this month was again one of severe flooding around the rivers draining the Himalaya where the monsoon rains continue to be frequent and heavy. On the 1st there were reports of 18 deaths around Darjeeling as a result of huge landslides. In the extreme north-east 14 were reported killed by a landslide on the 5th. On the 8th a landslide swept away two villages in Nepal killing at least 28; the same day 40 were feared to have died in Himachal Pradesh as a result of flash flooding. On the 10th scores were killed in Assam, Gujurat, Punjab and Uttar Pradesh and also in Kashmir. The 11th was no better and some were said to have been killed when the roofs of the houses collapsed under the downpour. On the 13th flood peaks had generally passed but forecasts of more rain soon gave no room for cheer. On the 16th fresh floods in the Punjab claimed 34 lives and 50 villages. On the 18th the Indus town of Sukkur reported heavy rain with 'storm force winds'; floodwater was knee-deep and further rain was expected. The 20th brought further reports of flooding; this time in Assam and West Bengal, the latter's excuse was that 790 mm of rain had fallen in the last 24 hours! Next day the focus was further north as it became clear that Kathmandu, and many other towns, were cut off from the rest of Nepal. In Bangladesh lightning was claiming dozens of lives about this time. In the Punjab 314 mm is said to have fallen in 24 hours to the 22nd and the whole of north-east India was cut off from the rest of the country. There were floods as far away as Rajastan, which is normally pretty dry. The port of Chittagong became unusable from the 23rd to the 25th as the floodwaters in the Karnaphuli river were augmented by a massive discharge from the Kaptai hydroelectric dam to prevent it becoming flooded as the water rose to 20 ft above normal. On the 25th the river Sutlej broke its banks in the Punjab adding to the disaster that had already befallen the area. It was about this time that the threat of a cholera epidemic became apparent. Almost half of Bangladesh was under water then but the worst seemed to be over by the end of the month for the whole region. However, heavy rain continued in the west, triggering more flash floods in Maharashtra State. In states south of the flood zones the reverse has occurred and many mid-eastern states suffered drought and crops suffered. By the end of the month the Indian death toll was about 1100, Nepal 3000 Bangladesh 400, total 4500 with more than six million displaced and short of food and safe water.

On a lighter note, the test match between Sri Lanka and India at Kandy (cricket of course) was abandoned with only 50 minutes play possible out of the five days to the 22nd — apparently this equals the record for the shortest test ever.

Africa (except the north coast)

The following notes are kindly supplied but the South African Weather Bureau.

Over most of South Africa it was the eighth consecutive month with below average rainfall, but it was very wet around the Cape. Here the period 6th to 14th saw a series of cold fronts bringing prolonged rain leading to the worst flooding for several years: 460 mm fell in five days near Goudini so that by the second week both the Berg and Breede rivers were in flood with the highest levels in 50 years. Problems were compounded on the 9th by storms over the Peninsula which blocked drains with hail: Nowlands collected 169 mm of rain that day which was so stormy that Cape Town harbour had to be closed. Another big hailstorm moved north across Durban on the evening of the 29th causing considerable damage and disruption. Although the highest temperature reported was 33.3 °C at Skukza on the 10th, the season was confirmed by a night minimum of −9.0 °C on the 30th at Buffelsfontein and snowfall on the Southern Cape mountains until the 19th.

Europe, North Africa and Arabia

On the 6th Meteosat images showed a large Cb approaching Bordeaux and our ATD lightning detectors showed it to be electrically very active. Its passage eastwards across France left a trail of devastation. Two were drowned and 60 had to be rescued from rivers transformed into torrents; hailstones the size of tennis balls fell on an open-air concert at Vienne injuring a dozen (one had a fractured skull). The same report wrote that much of Beaujolais wine crop was damaged.

After the rains earlier this year swarms of locusts are reported to have crossed the Red Sea into Yemen causing the customary devastation to crops in their path.

Throughout the month rain fell heavily over the Ukraine leading to severe flooding in the north and to at least six deaths. By the end of the month conditions were beyond local control and foreign help was being sought. Neighbouring Belarus (Belorussia) also suffered badly, with flooding being especially severe in the south with 2 million tonnes of grain and half the potato crop under threat. Flood damage was put at $35m.

July tropical storms

This is a list of tropical storms, cyclones, typhoons and hurricanes active during May 1993. The date are those of first detection and date of falling out of the category through dissipation or becoming extratropical. The last column gives the maximum sustained wind in the storm during this month. The maps show 0000 UTC positions: for these I must thank Julian Heming and Susan Coulter of the Data Monitoring group of the Central Forecasting Office.

No	Name	Basin	Start	End	Max. (kn)
1	Calvin	NEP	4 Jul	8 Jul	90
2	Dora	NEP	14 Jul	21 Jul	110
3	Eugene	NEP	16 Jul	25 Jul	110
4	Lewis	NWP	7 Jul	12 Jul	85
5	Marian	NWP	13 Jul	17 Jul	45
7	Ofelia	NWP	25 Jul	28 Jul	45
8	Percy	NWP	27 Jul	30 Jul	75

Basin code: N — northern hemisphere; S — southern hemisphere; A — Atlantic; EP — east Pacific; WP — west Pacific: I — Indian Ocean; WI — west Indian Ocean; AUS — Australasia.

Cyclone Konita followed a hook-shaped course to SW, S and finally NNE. Adele did a lot of damage on the Trobriand Islands off New Guinea.

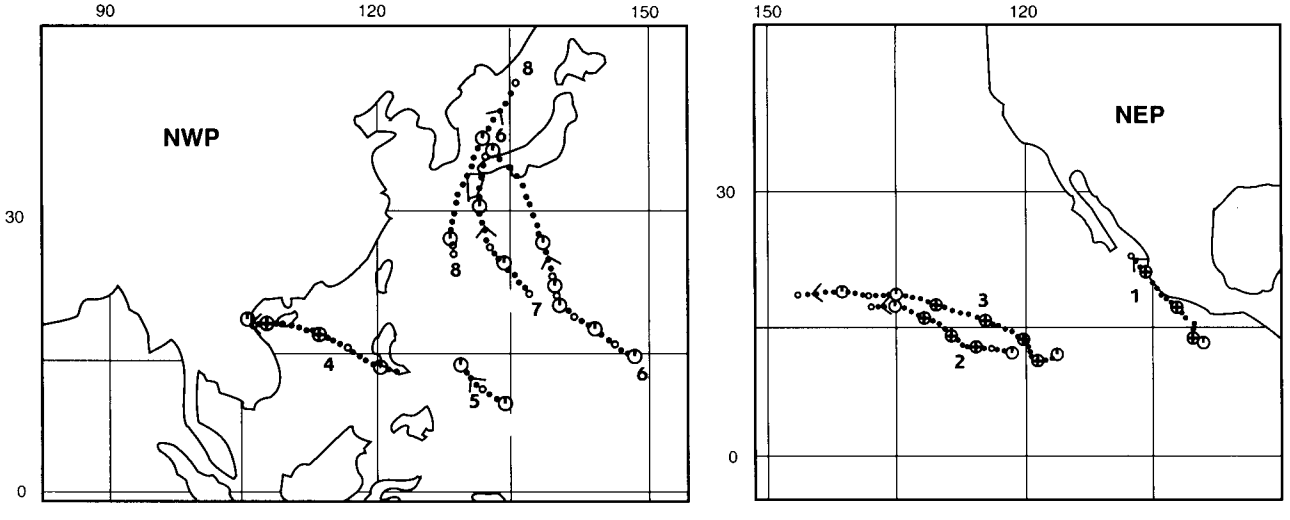

The publication of the *Meteorological Magazine* will cease with the issue for December 1993.

The December 1993 issue of the *Meteorological Magazine* will be a bumper one of about 40 pages celebrating the Magazine's contribution to the development and dissemination of meteorological knowledge. It will contain a selection of highlights from 1866 up to around 1986.

The first edition of the *Meteorological Magazine* was published in 1920 by HMSO. It took over from *Symons's Meteorological Magazine* which started in 1866. This decision therefore brings to an end a continuous publishing record of 129 years (except for the duration of World War 11). It is understood that legal obligations accepted when *Symons's Meteorological Magazine* was adopted are fulfilled by the continuing production of the *Monthly Weather Report* and *Rainfall 19XX* and our internal journal mentioned
below.

As one of the leading European establishments for research into meteorology, our publications should be subject to external peer review: this is already the case for much Meteorological Office work. The publication of a new international and European quarterly journal by the Royal Meteorological Society (called *Meteorological Applications*) provides a suitable vehicle for most kinds of articles that have appeared in *Meteorological Magazine*, namely on research, practice, measurements, reviews articles, applications of meteorology, book reviews, etc. Enquiries should be addressed directly to the Royal Meteorological Society.

The United Kingdom Meteorological Office (UKMO) Annual Scientific and Technical Review 1993/94

This Review describes the major developments in science and technology within the UKMO over the year April 1993 to March 1994 and is produced as part of the Meteorological Office Annual Report and became available in July 1994. If you wish to be put on the mailing list for future years please write to:

The News Desk, Publications (room 707a), Meteorological Office, London Road, Bracknell, Berks RG12 2SZ.

If you want a copy of this year's Technical Review, please see the Editorial on page 247.

Informal communications

The UKMO has instituted an in-house periodical for informal and rapid dissemination of the latest relevant science and technology news to its staff and outside collaborators. Most contributions come from UKMO staff, but offers of material from outside will be welcome — though there is no guarantee of publication.

Back numbers

Limited stocks of back numbers from 1970 to date are available from:
Vic Silk, The Library, Meteorological Office, London Road, Bracknell, BERKS, RG12 2SZ; telephone 01344 854074.
Copies cost £1.50 each (inclusive). Please send sterling cheques made out to 'Public sub-account HMG 4712'; leave the amount blank but cross them and endorse with the maximum so that the transaction can be made even if some of the requested issues sell out. Please send an addressed label with the order. Remaining stocks will be disposed of in March 1995.

Full-size reprints of Vols 1–75 (1866–1940) are available from Johnson Reprint Co. Ltd., 24–28 Oval Road London NW1 7DX.

Complete volumes of *Meteorological Magazine* commencing with volume 54 are available on microfilm from University Microfilms International, 18 Bedford Row, London WC1R 4EJ. Information on microfiche issues is available from Kraus Microfiche, Rte 100, Milwood, NY 10546, USA.

October 1993

Edited by R.M. Blackall
Editorial Board: R.J. Allam, N. Wood, W.H. Moores, J. Gloster, C. Nicholass, G. Lupton, F.R. Hayes

Vol. 122
No. 1455

Contents

ISSN 0026—1149

Dd 291241 9/94 C12 543 24530